Neutron Scattering studies of the Crystal and Magnetic Structures of Molecular Magnets

Danielle Villa
Mentors: Craig Brown and Qingzhen Huang

Molecular Magnets

- Molecular Quantum Magnets
  - Molecules that exhibit magnetic behavior at low temperatures
    - Antiferromagnetism ↓ ↑ ↓ ↑
- $\hat{H} = \sum D(\hat{S}_i^{z2}) + \sum J_{ij}\hat{S}_i \cdot \hat{S}_j$
  - D-> Single Ion Anisotropy
  - J-> Magnetic Exchange Interaction

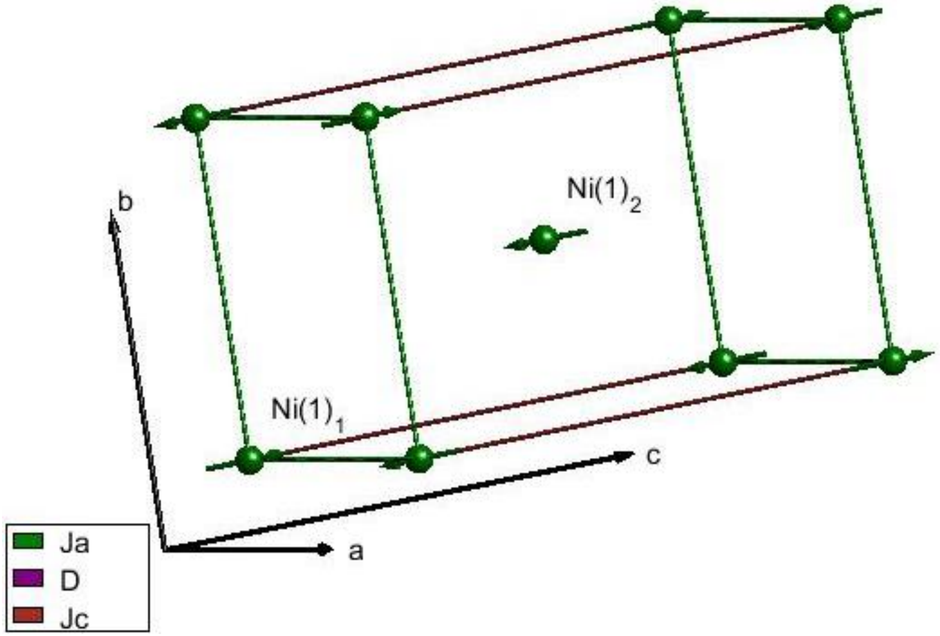

- Quantum Theory
- Information Storage
- Quantum Computing

Neutrons

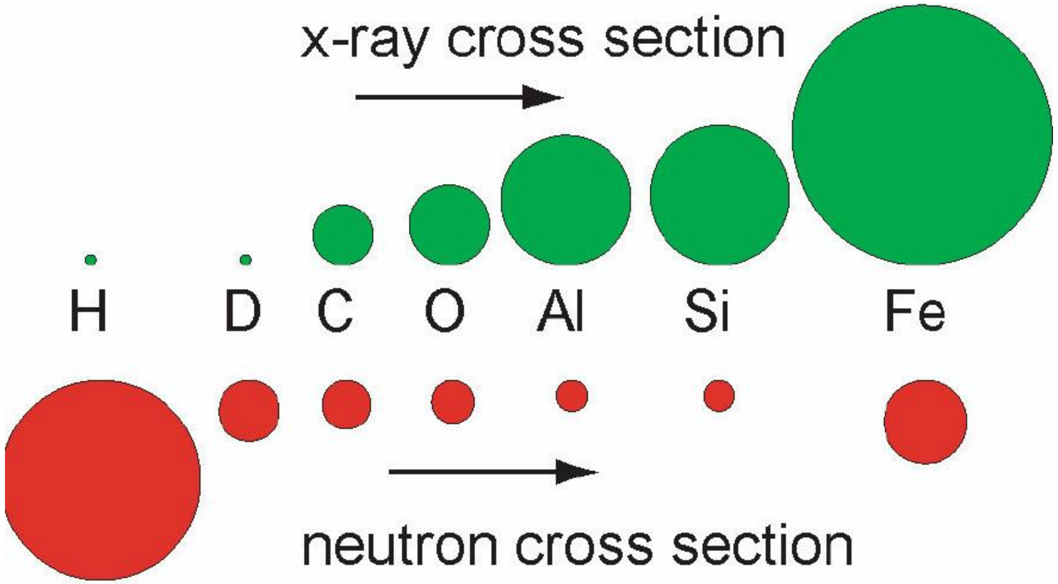

"Dynamics and Neutron Scattering" by John R.D. Copley

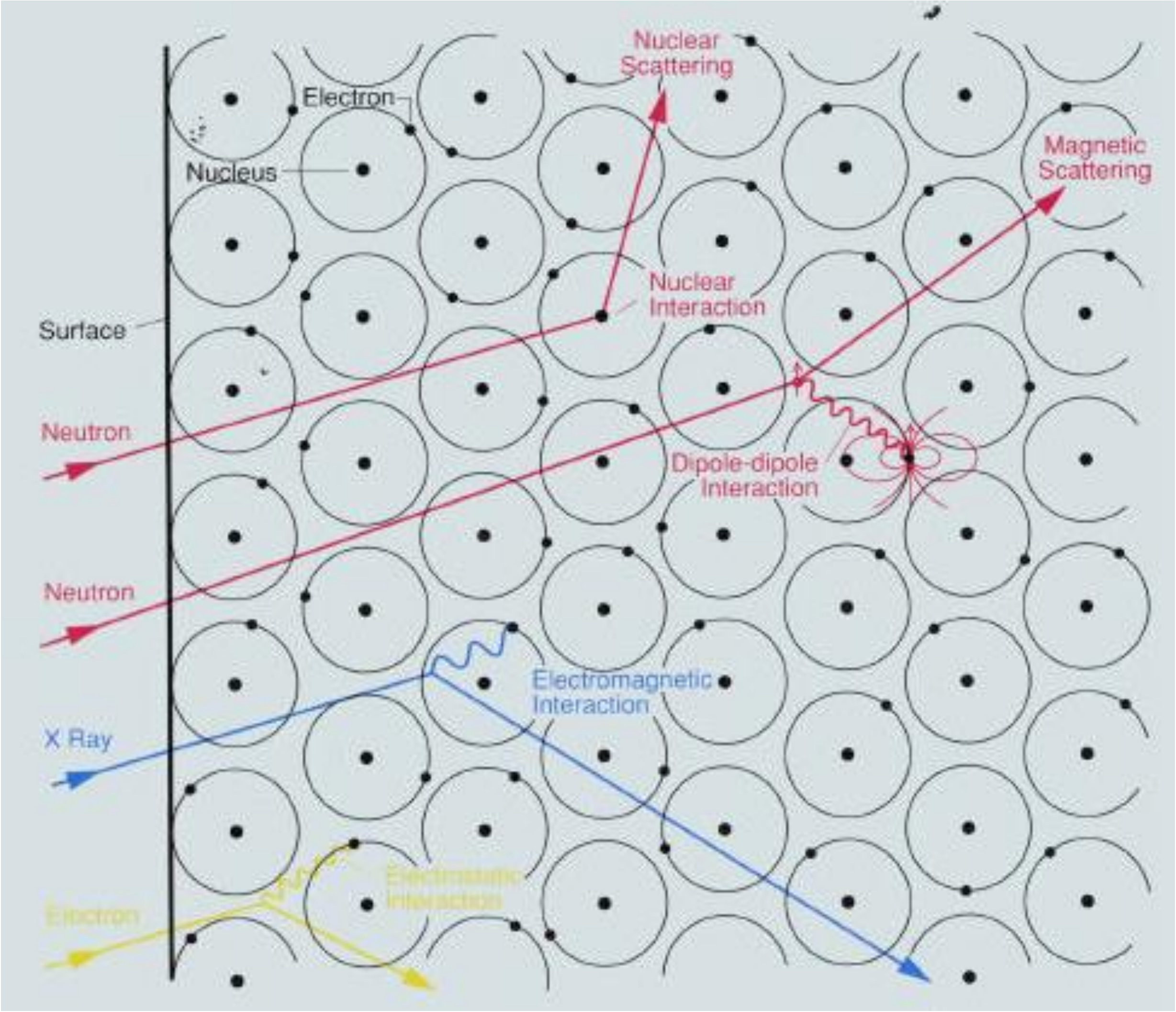

Neutron Scattering "LECTURE 1: Introduction & Neutron Scattering "Theory"" by Roger Pynn

Neutron Scattering

Diffraction

BT-1 High Resolution Powder Diffractometer

Inelastic

Disk Chopper Time of Flight Spectrometer

Powder Diffraction

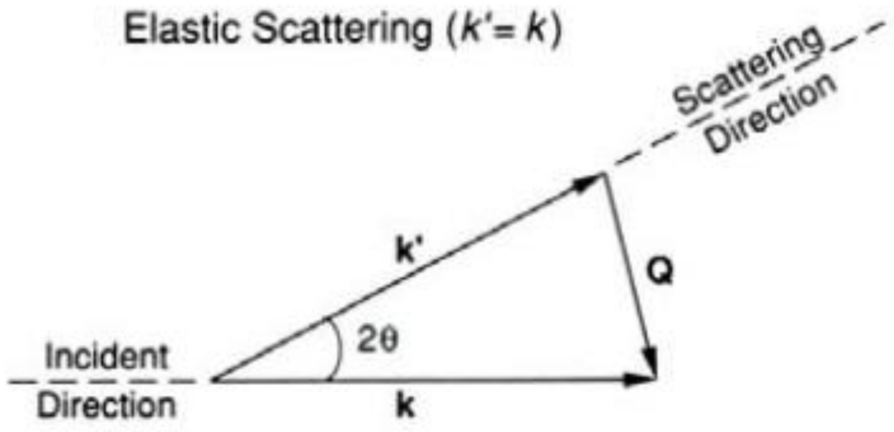

https://en.wikipedia.org/wiki/X-ray_crystallography

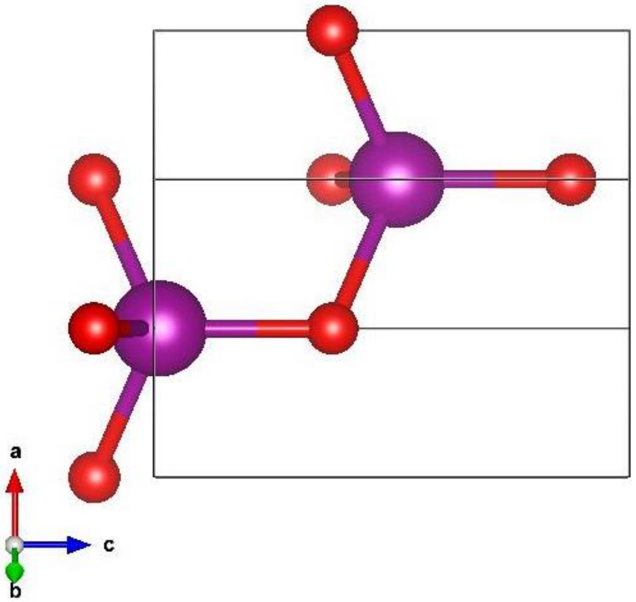

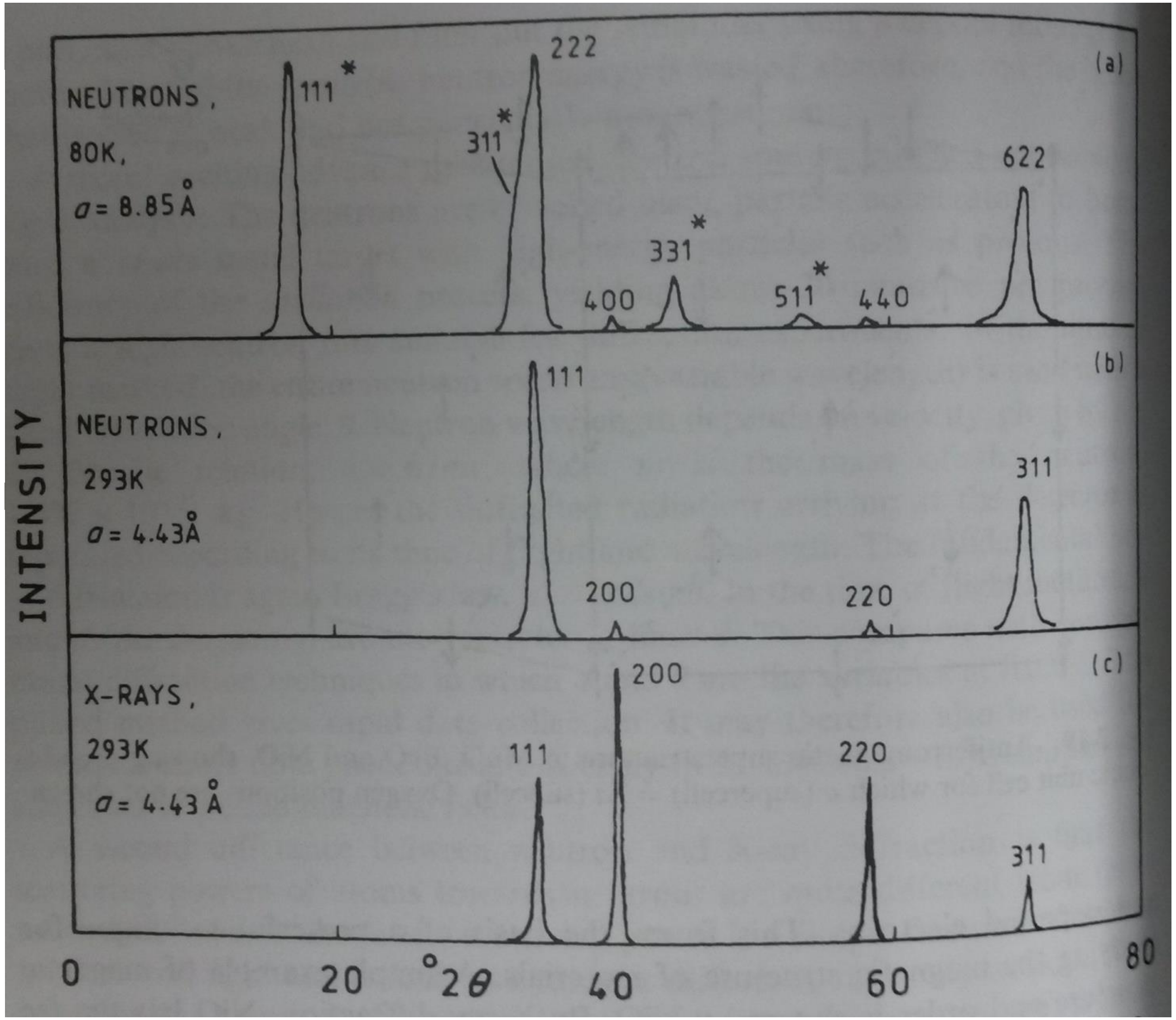

Basic Solid State Chemistry by Anthony R West (pg. 164)

Structure from Ki Min Nam, *et al. J. Am. Chem. Soc.*, **2012**, *134* (20), pp 8392–8395

$CoCl_2pyz_2$

- S = 3/2
- Orthorhombic
- T_N = 0.8 K

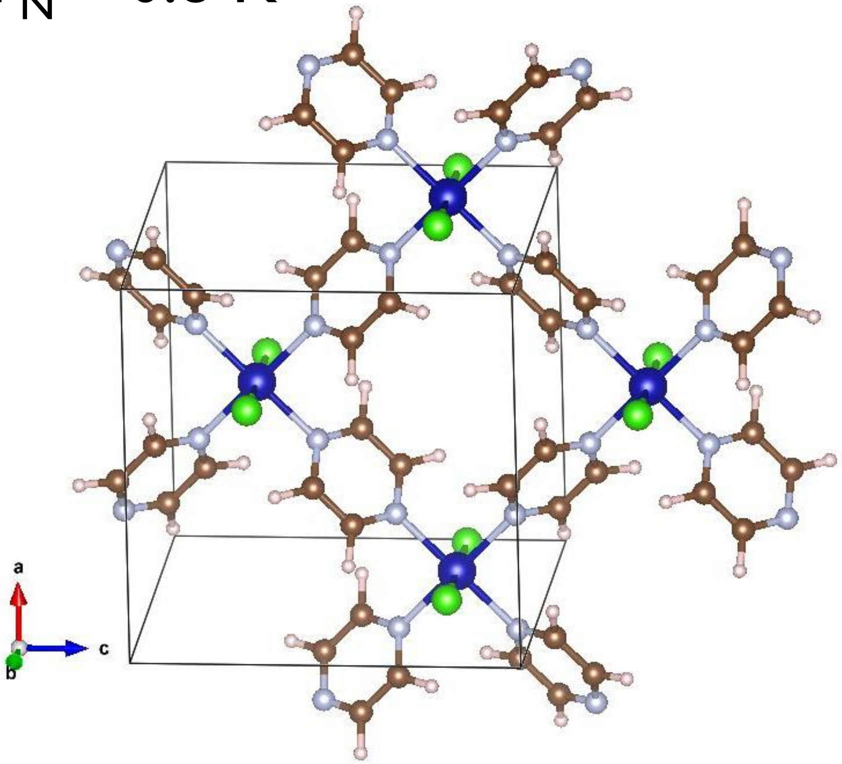

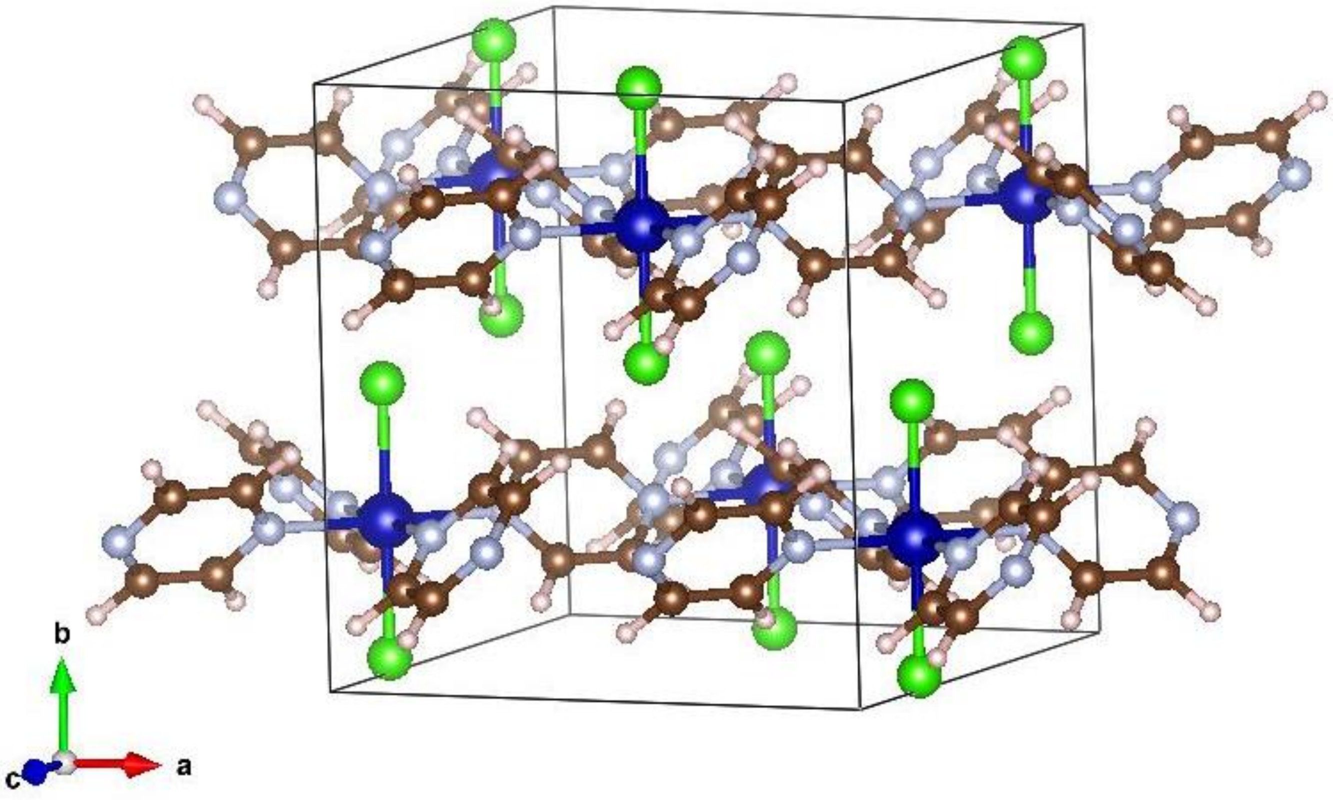

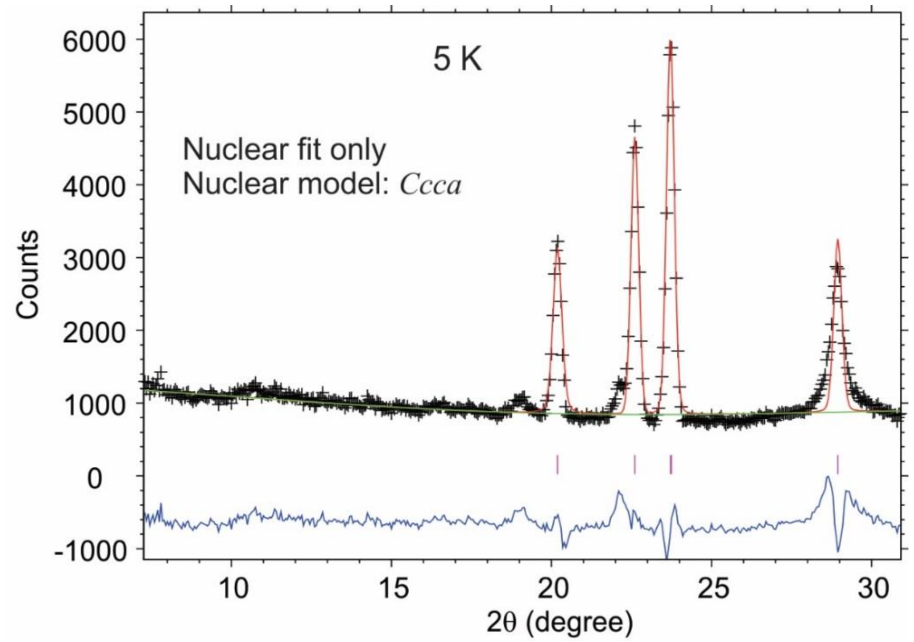

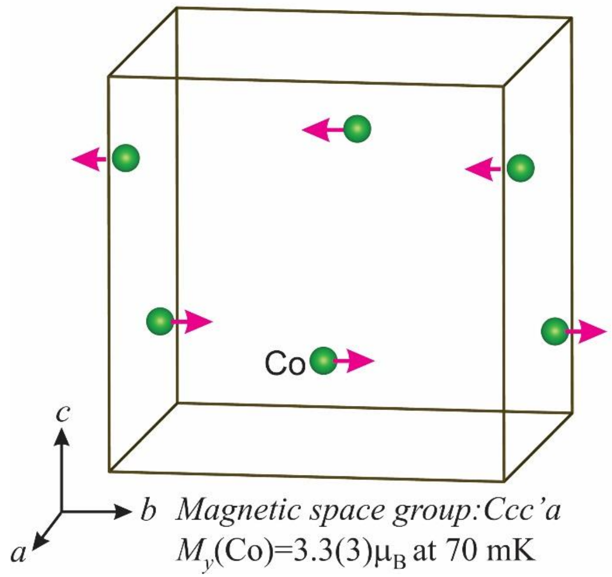

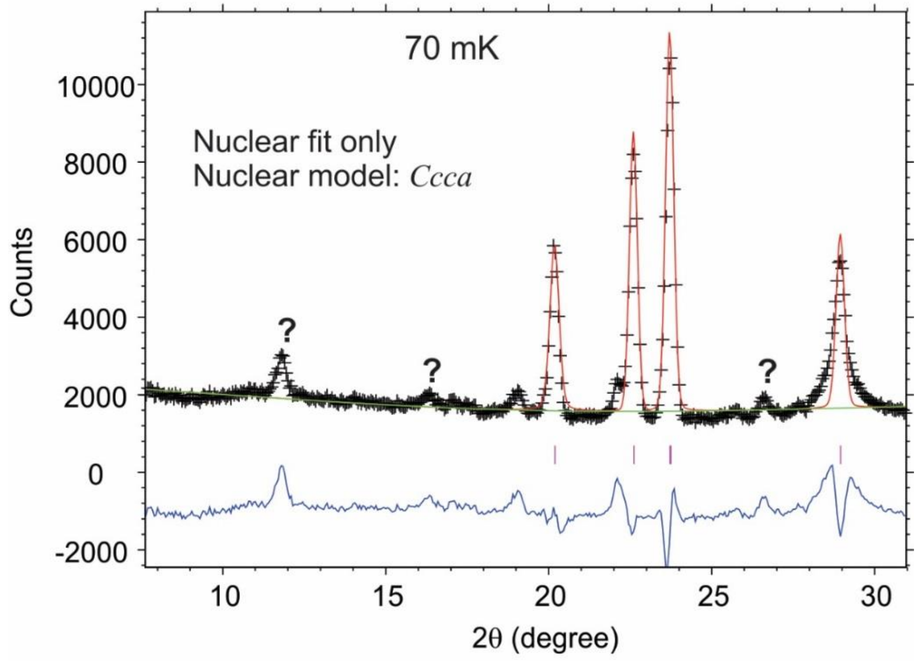

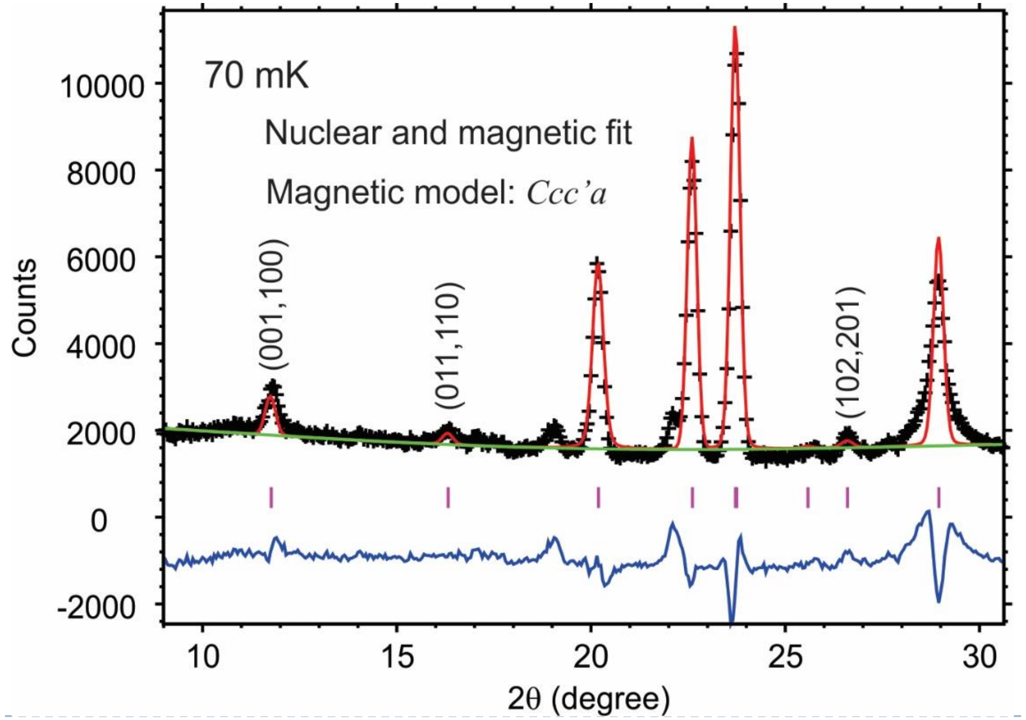

Unpublished Data
Fit by Qingzhen Huang

Inelastic Scattering

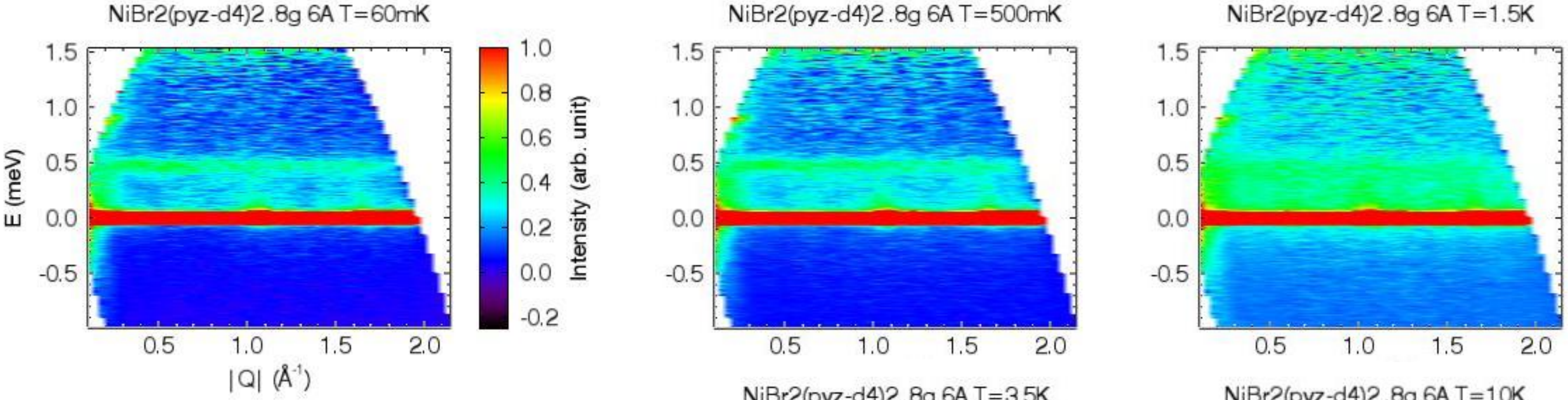

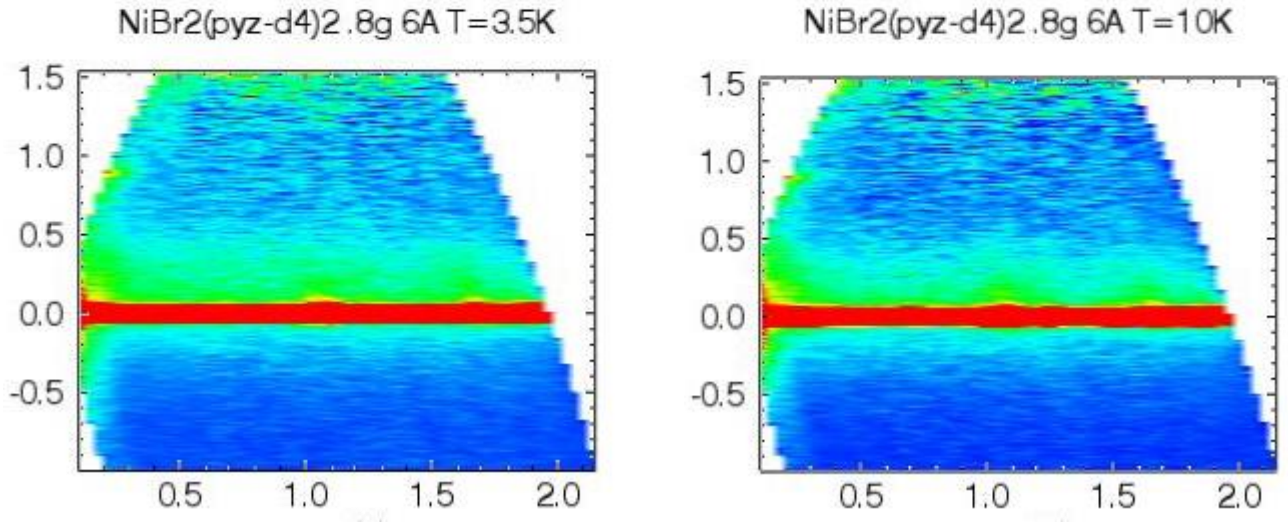

Neutron Scattering—A Non-destructive Microscope for Seeing Inside Matter
By Roger Pynn

$NiX_2(pyz)_2$

$NiCl_2(pyz)_2$

- S=1
- Tetragonal

$NiBr_2(pyz)_2$

- S=1
- Tetragonal

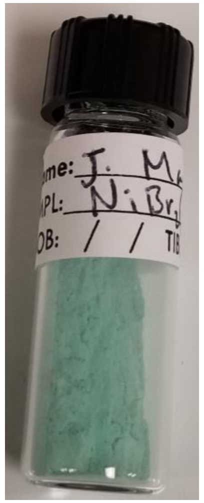

$NiX_2(pyz)_2$

Single Layer

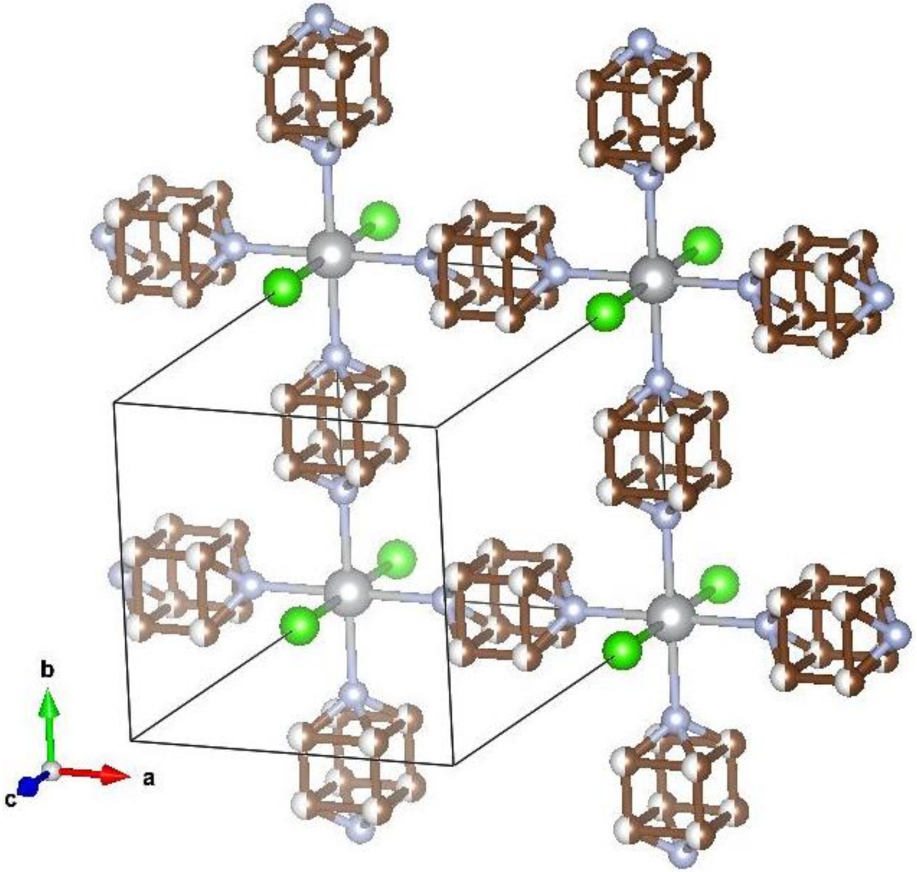

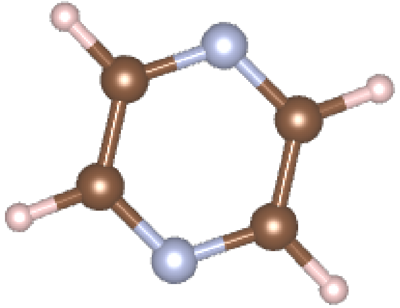

Pyrazine

Unit Cell

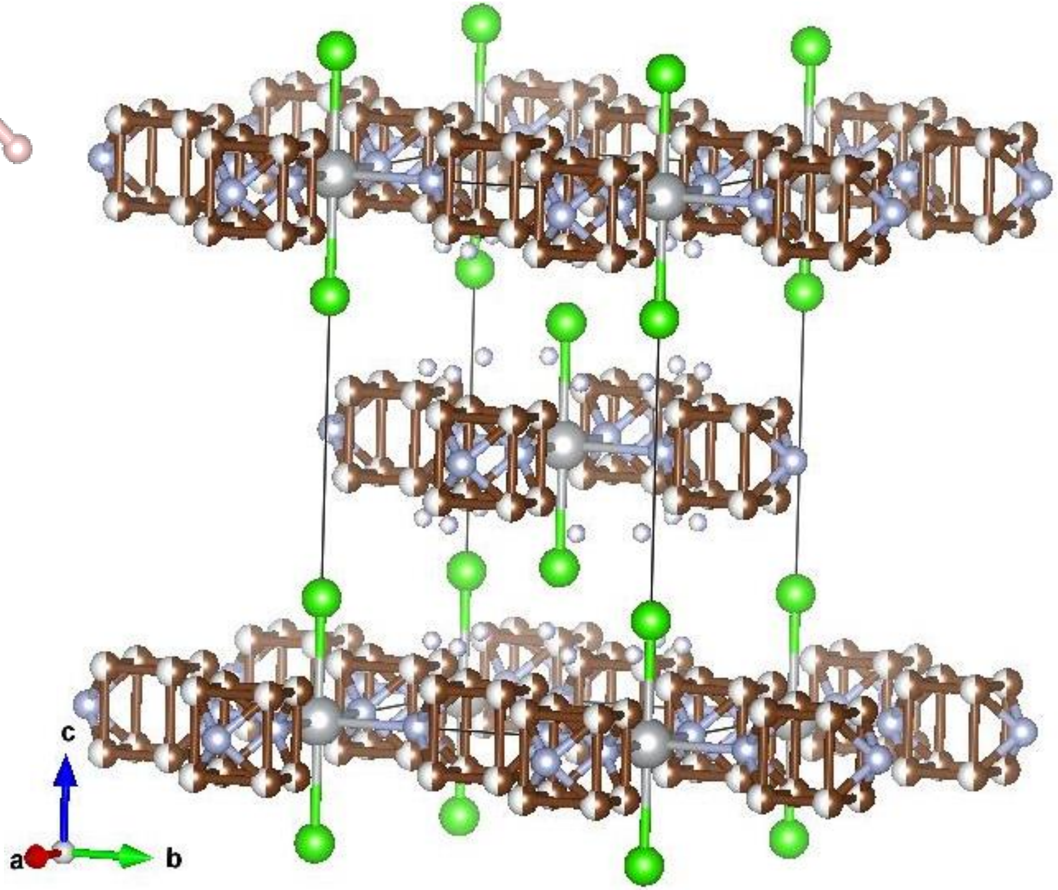

$NiX_2(pyz)_2$

$NiCl_2(pyz)_2$

- S=1
- Tetragonal

$NiBr_2(pyz)_2$

- S=1
- Tetragonal

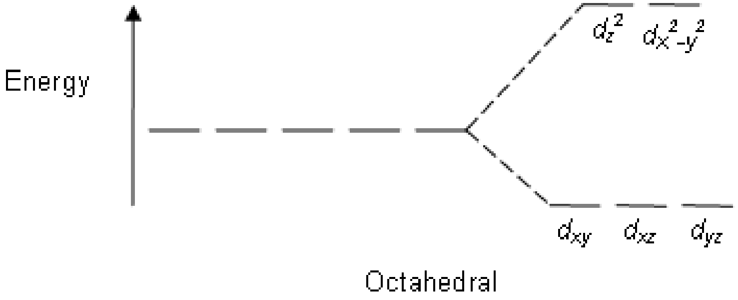

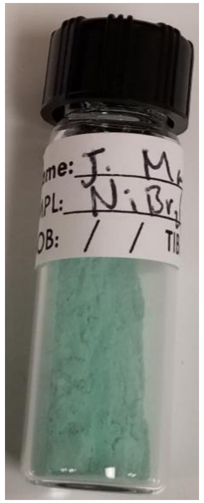

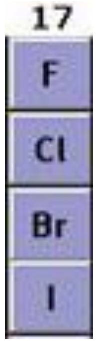

Long Range Magnetic Order

- $NiBr_2$
  - T_N = 1.9 K
- $NiCl_2$
  - T_N < 0.08 K

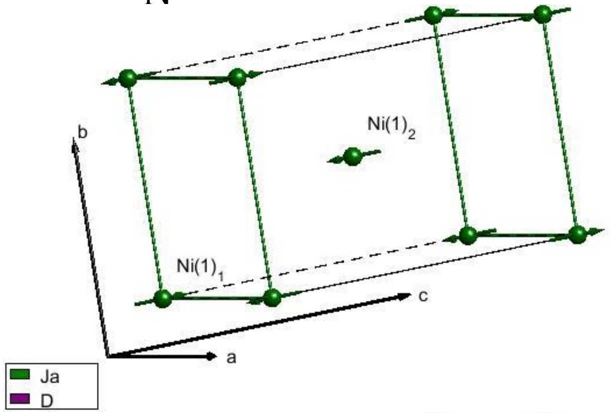

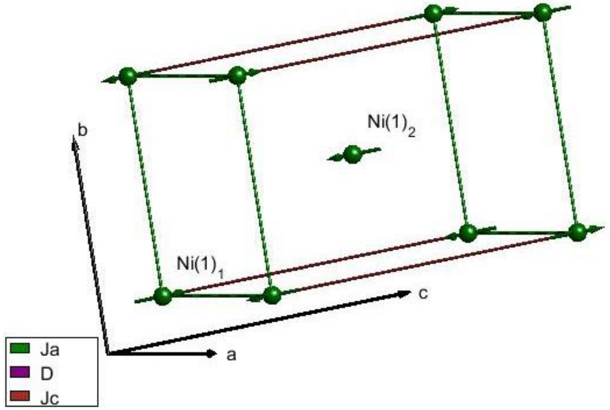

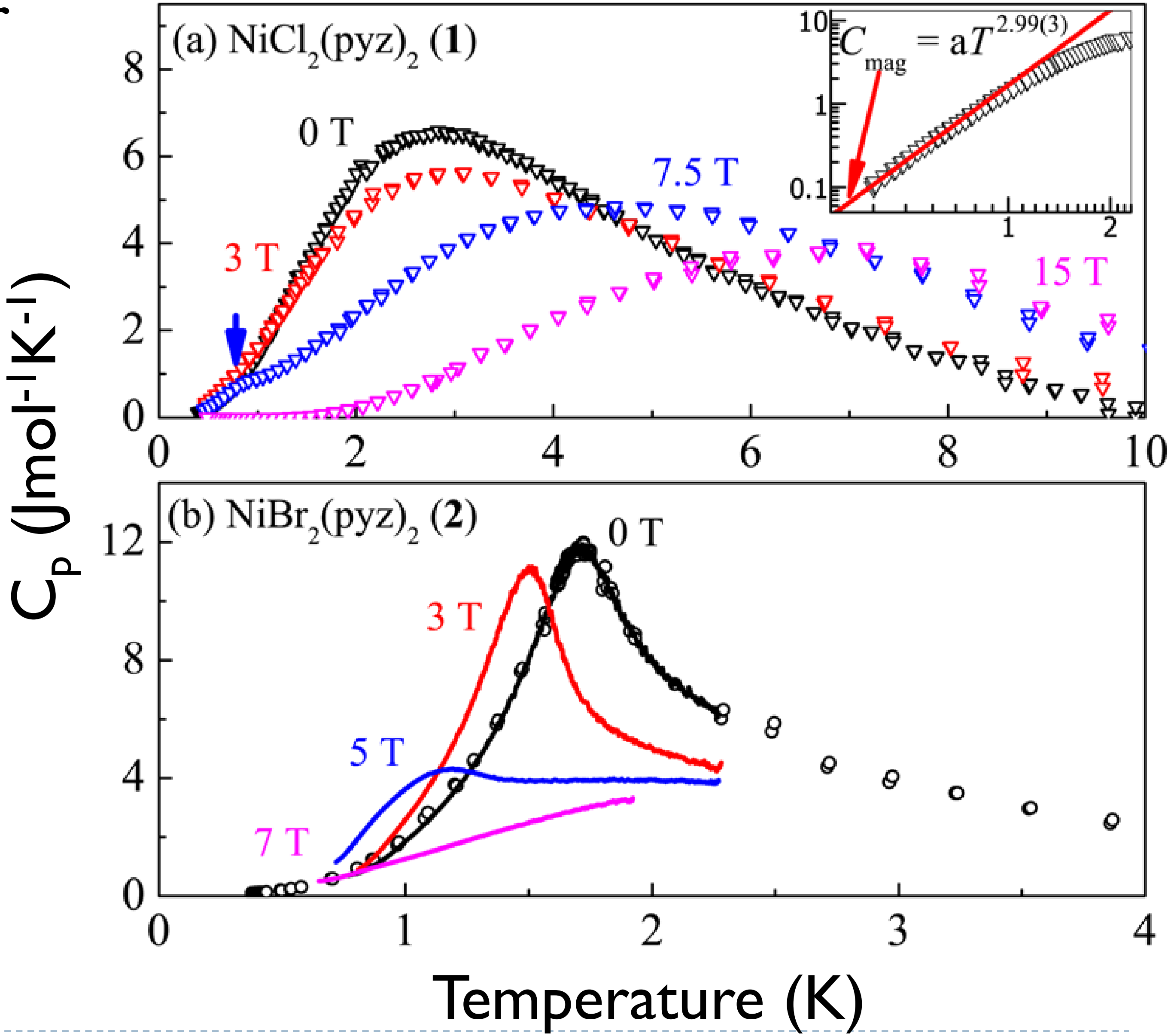

J. Liu, *et al.* Inorg. *Chem.* **2016**, *55*, 3515–3529

$NiBr_2pyz_2$

- S=1
- Tetragonal
- T_N=1.9 K

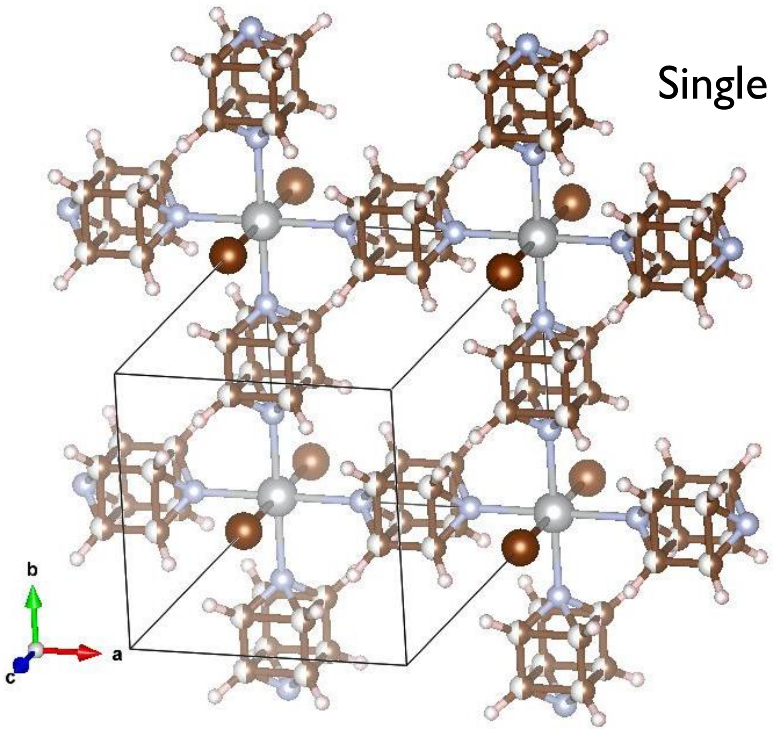

Single Layer

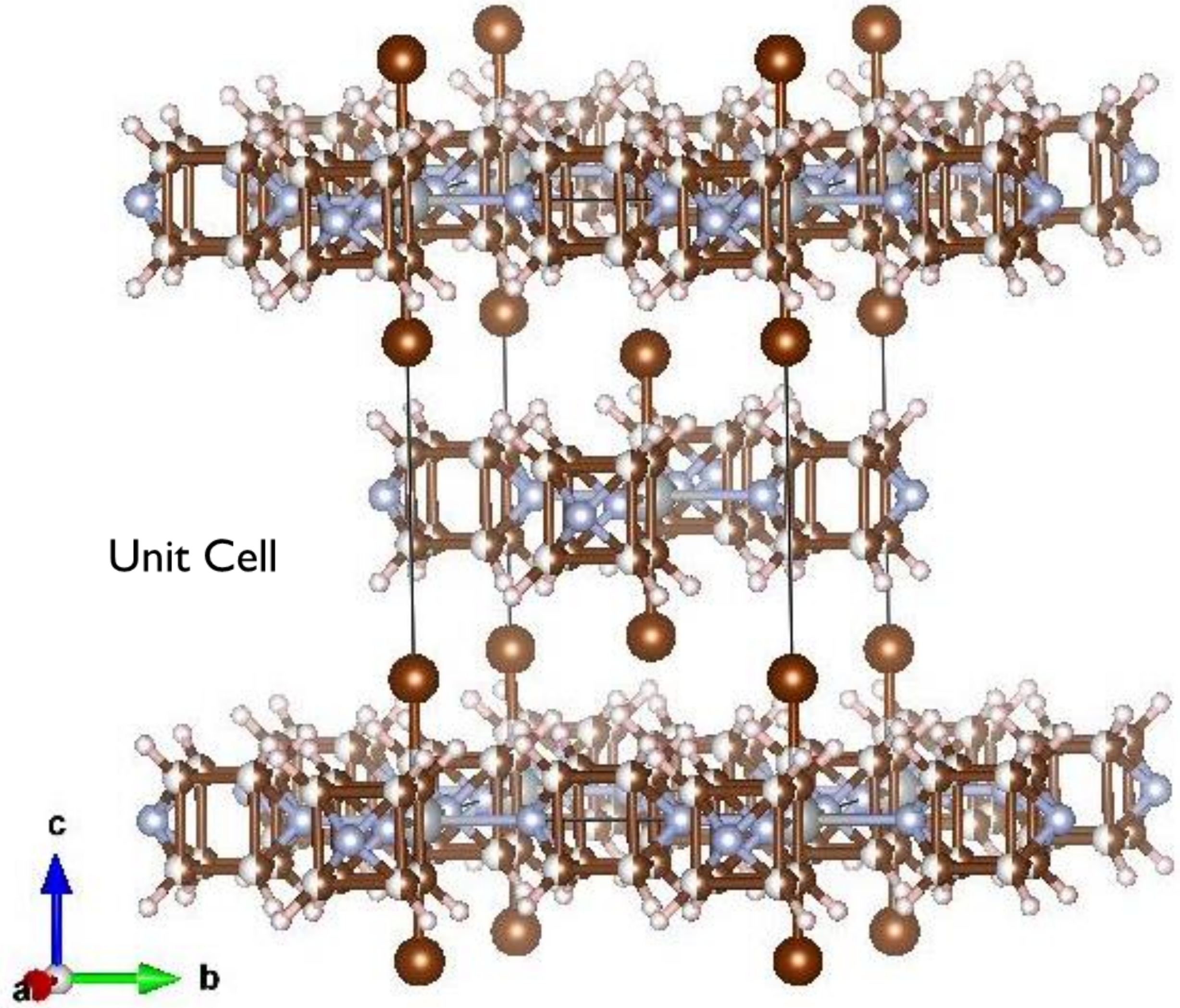

Unit Cell

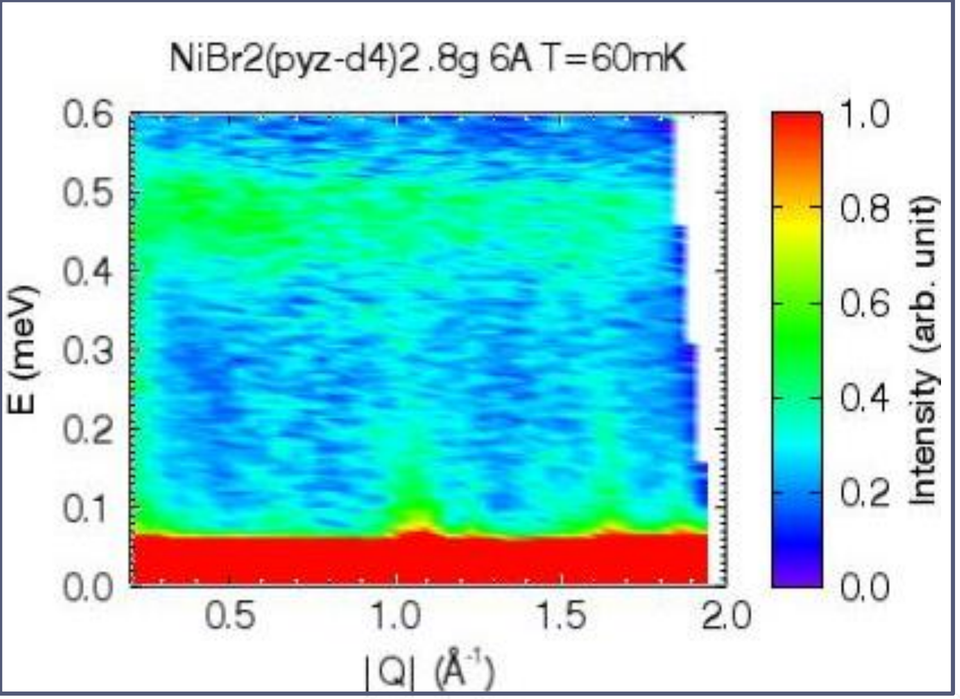

J=0.09 meV D=0 meV

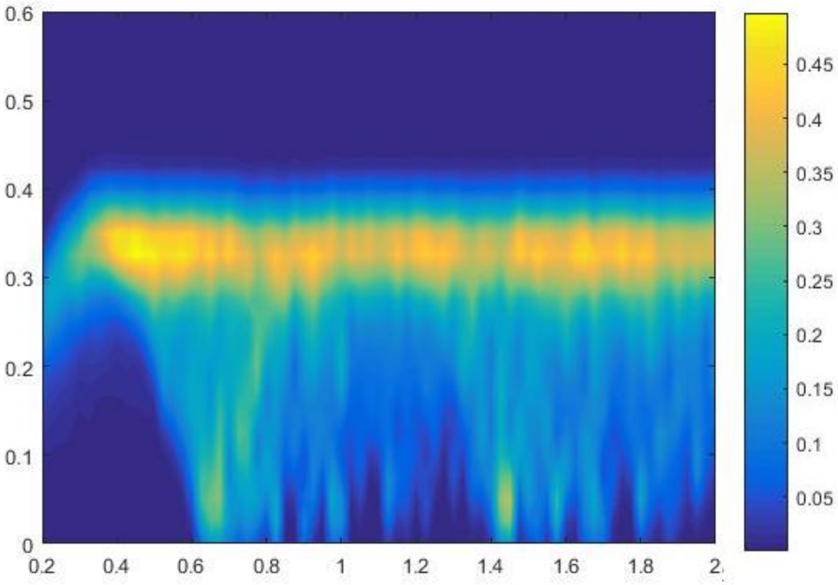

J=0.09 meV D=0 meV J'=0.02 meV

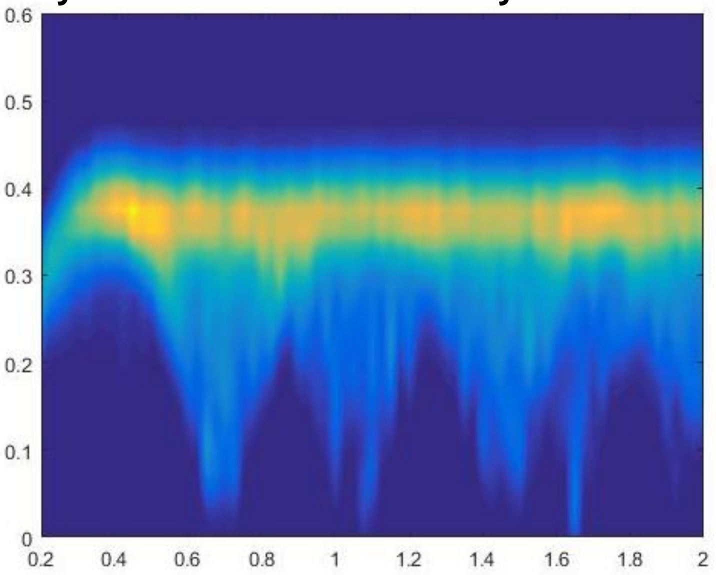

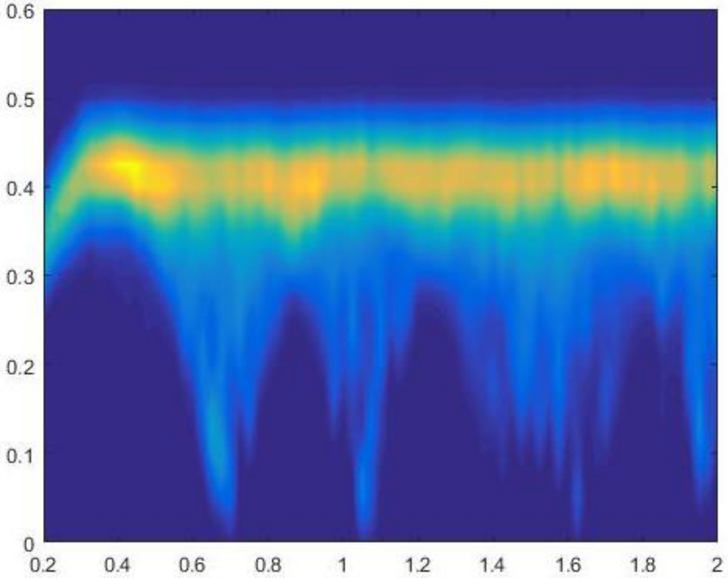

J=0.09 meV D=0 meV J'=0.04 meV

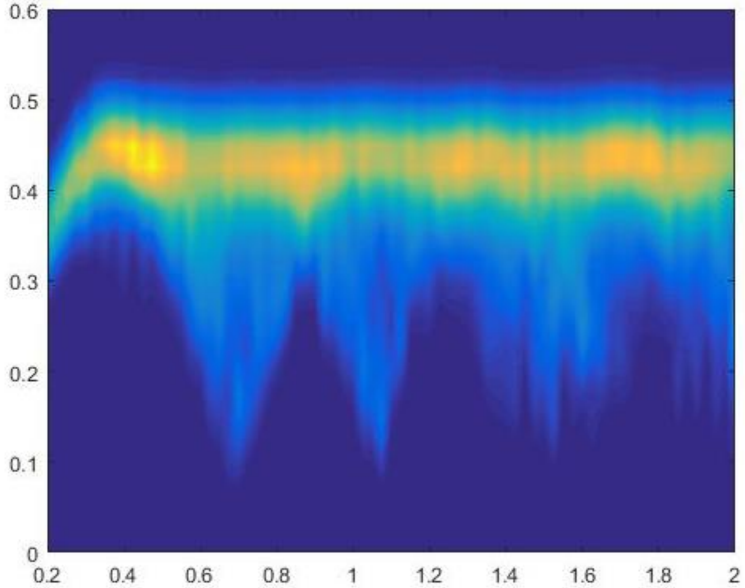

J=0.09 meV D=-0.009 meV J'=0.04 meV

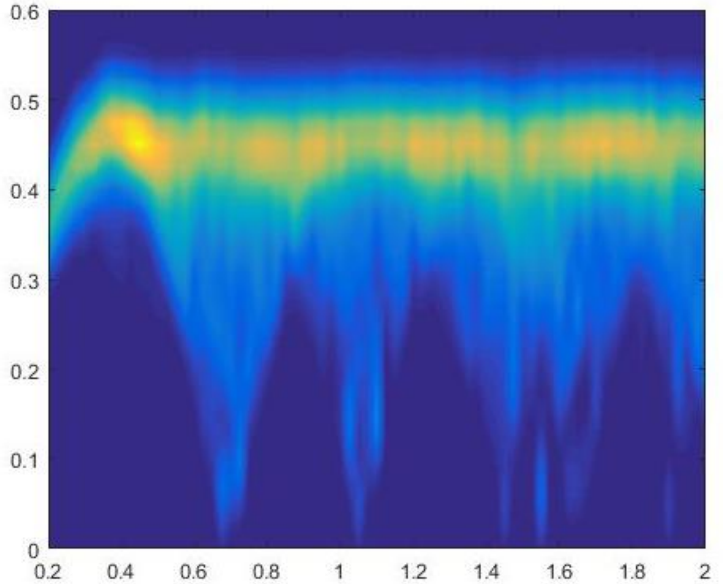

J=0.099 meV D=-0.0009 meV J'=.04 meV

A Need

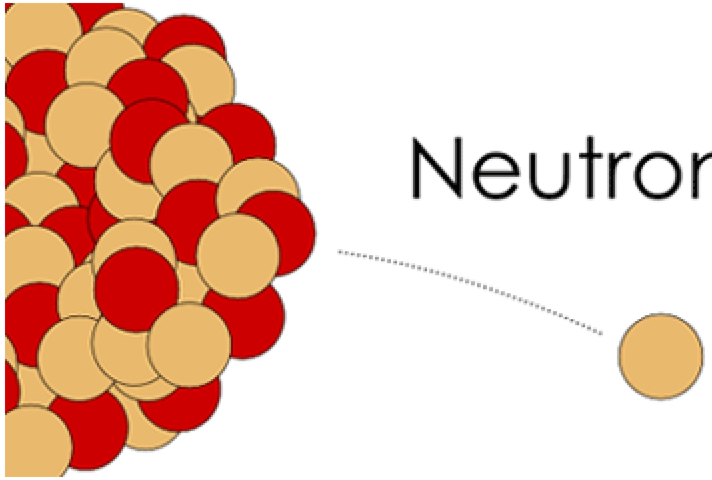
Neutron

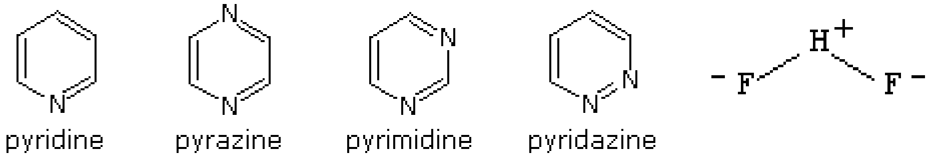
N
N
N
N
N
N
N
pyridine
pyrazine
pyrimidine
pyridazine
H+
- F
F -

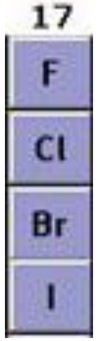
17
F
Cl
Br
I

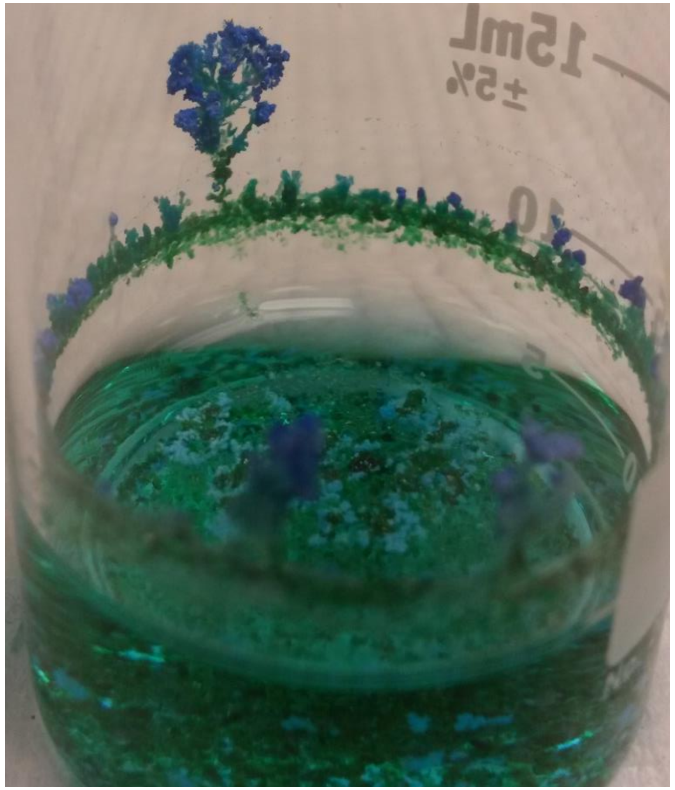
15ml
±5%

Thank You

- Qingzhen Huang
- Craig Brown
- Jamie Manson
- Joe Dura
- Julie Borchers
- Dan Neumann
- Steve Disseler
- William Ratcliff
- Juscelino Leao
- Yegor Vekhov
- Alan Ye
- Terry Udovic
- Jeff Lynn
- Yamali Hernandez
- Jamie Brambleby
- Paul Goddard

Non-NIST Experimental Partners

- The University of Warwick
- Advanced Photon Source, Argonne National Laboratory
- National High Magnetic Field Laboratory, Los Alamos National Laboratory
- Swiss Muon Source, Paul Scherrer Institut
- ISIS Pulsed Neutron and Muon Source

Software Used for Data Analysis

- Neutron Diffraction
  - CMPR
  - GSAS
- Inelastic Neutron Scattering
  - DAVE
  - SpinW
- Visualization
  - VESTA

$CoCl_2pyz_2$

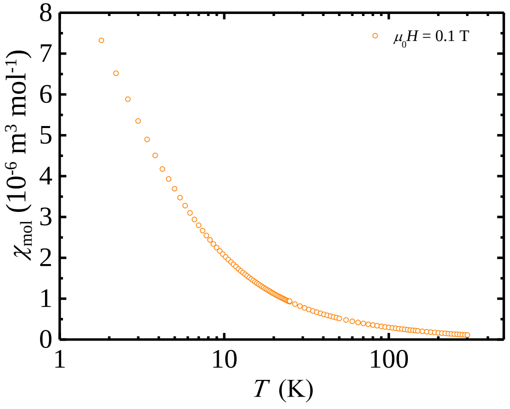

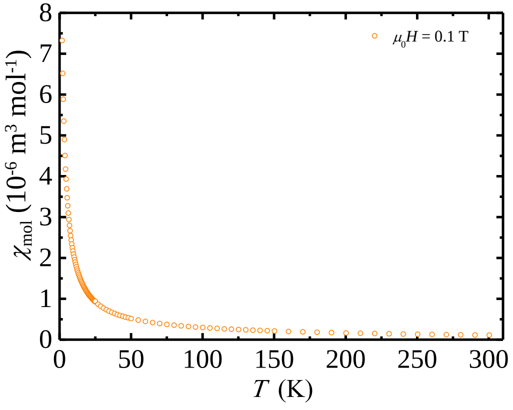

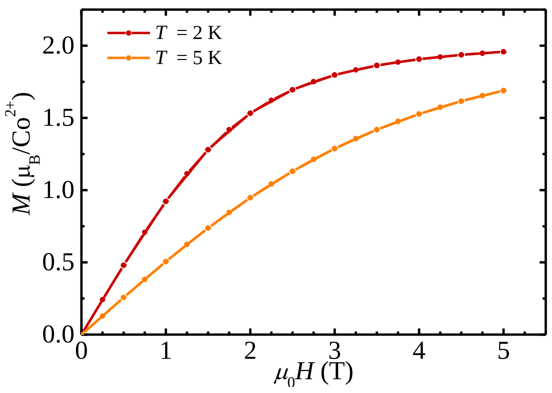

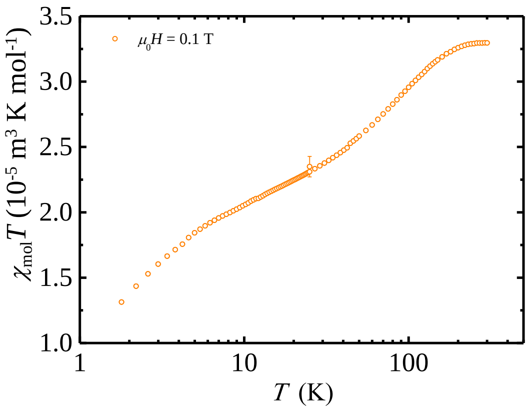

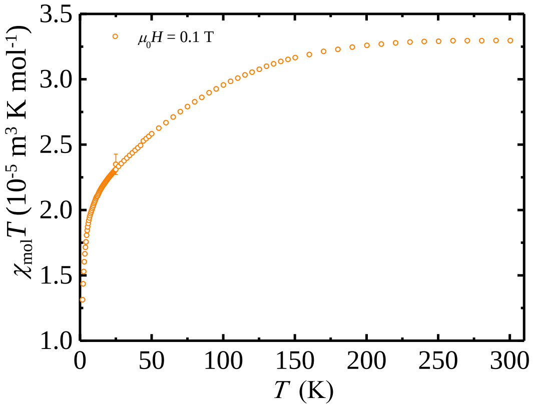

JLM4-088: $CoCl_2(pyz\text{-}D_4)_2$

Sample dispersed in Vaseline

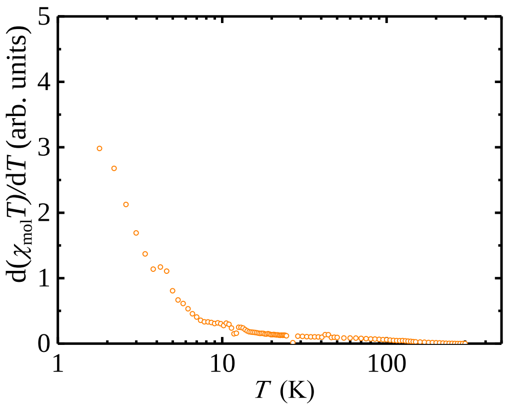

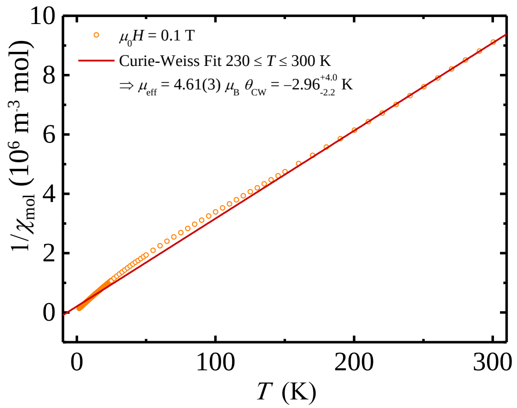

Comparison:

Sample *without* Vaseline

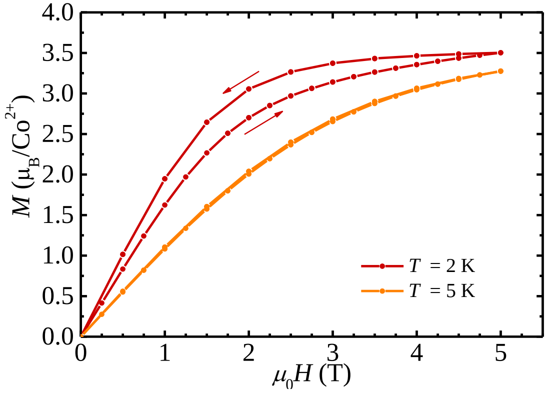

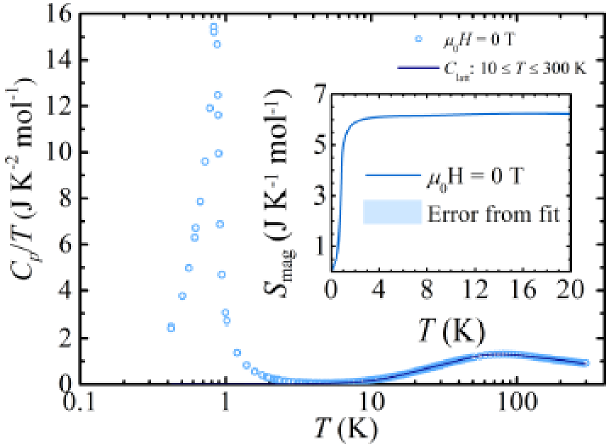

Fig. 1 Heat capacity (plotted as C_p/T) vs. temperature for $Co_2Cl_2(pyz\text{-}d_4)_2$ (JLM4-088). A Peak at 0.85(1) K indicates a transition to long range order. The solid line is a fit to a model of one Debye plus two Einstein modes in the range 10 ≤ T ≤ 300 K . Inset: Subtracting the lattice contribution from the data, the entropy change to 20 K is determined to be consistent with R ln 2 = 5.8 J K^{-1} mol^{-1}, indicating the sample behaves as an effective spin 1/2 system at low temperatures.

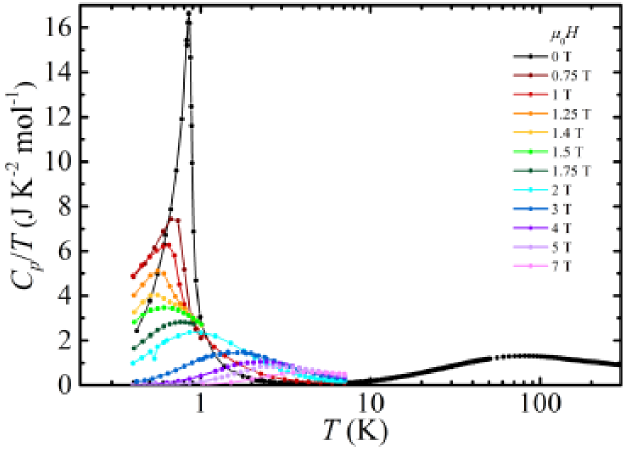

Fig. 3 Field dependence of C_p/T vs. T. The λ-peak moves to lower temperatures as the field is increased, indicative of a transition to an AFM ordered ground state. T_N is too low to be experimentally accessible for applied fields μ_0H ≥ 1.5 T. At higher fields a broad feature emerges which moves monotonically to higher temperatures with applied field.

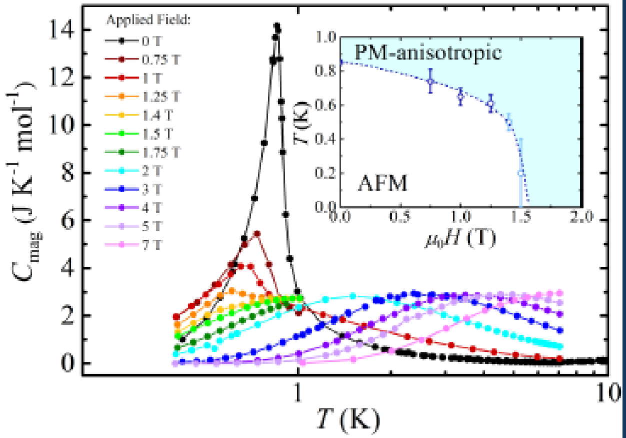

Fig. 4 Magnetic heat capacity (C_{mag}) vs. T, following subtraction of the lattice fit. The broad feature (for μ_0H ≥ 3 T) has a constant amplitude, and a peak position which increases linearly with field. This is highly indicative of a Schottky anomaly due to the field-induced splitting of the doublet ground state in Co^{2+}. Inset: phase boundary separating the paramagnetic state (with easy-plane anisotropy) with the AFM ordered state. Faded points are most easily seen in C_p/T vs. T (Fig. 3).

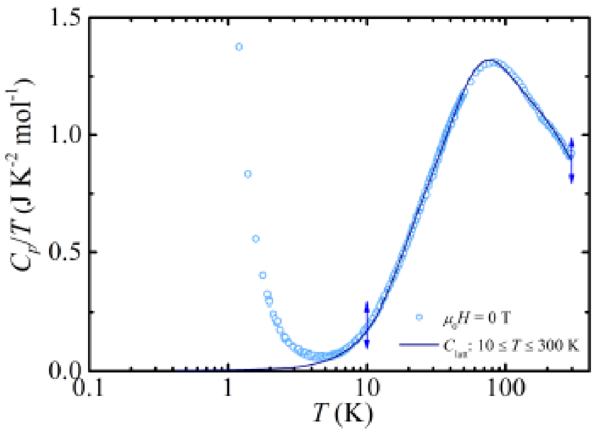

Fig. 2 Heat capacity vs. temperature, showing the lattice fit to the data. The fit only has a small dependence on the lower bound used for the fit, giving rise to the small error in the calculated entropy change (Fig. 1 Inset).

Fig. 5 Simulated molar heat capacity (C_{mag}) vs. T, for a two level system in an applied field. The result is a Schottky anomaly, with the equation given in the figure. The g-factor was taken to be the powder average g-factor, assuming the published[1] values for the fully hydrogenated phase of g_{xy} = 5.98 and g_z = 1.97. This model is a good representation of the measured data (Fig. 4), having the approximately the correct amplitude and field dependence for the maxima.

[1] R. L. Carlin *et al.*, *PRB* **32**, 7476 (1985).

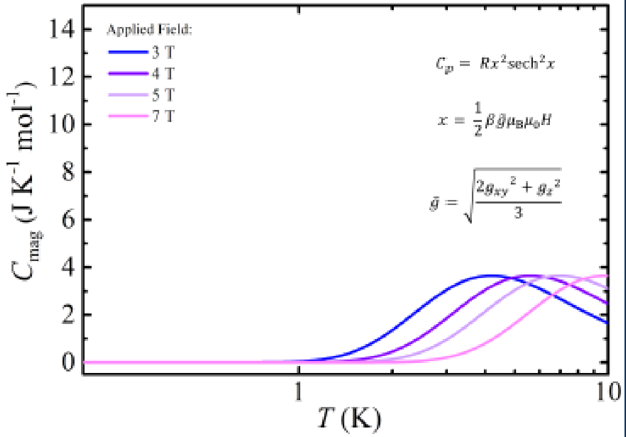

$CoCl_2(pyz\text{-}d_4)_2$ (Bacth #: JLM4-088) 22nd May 2015

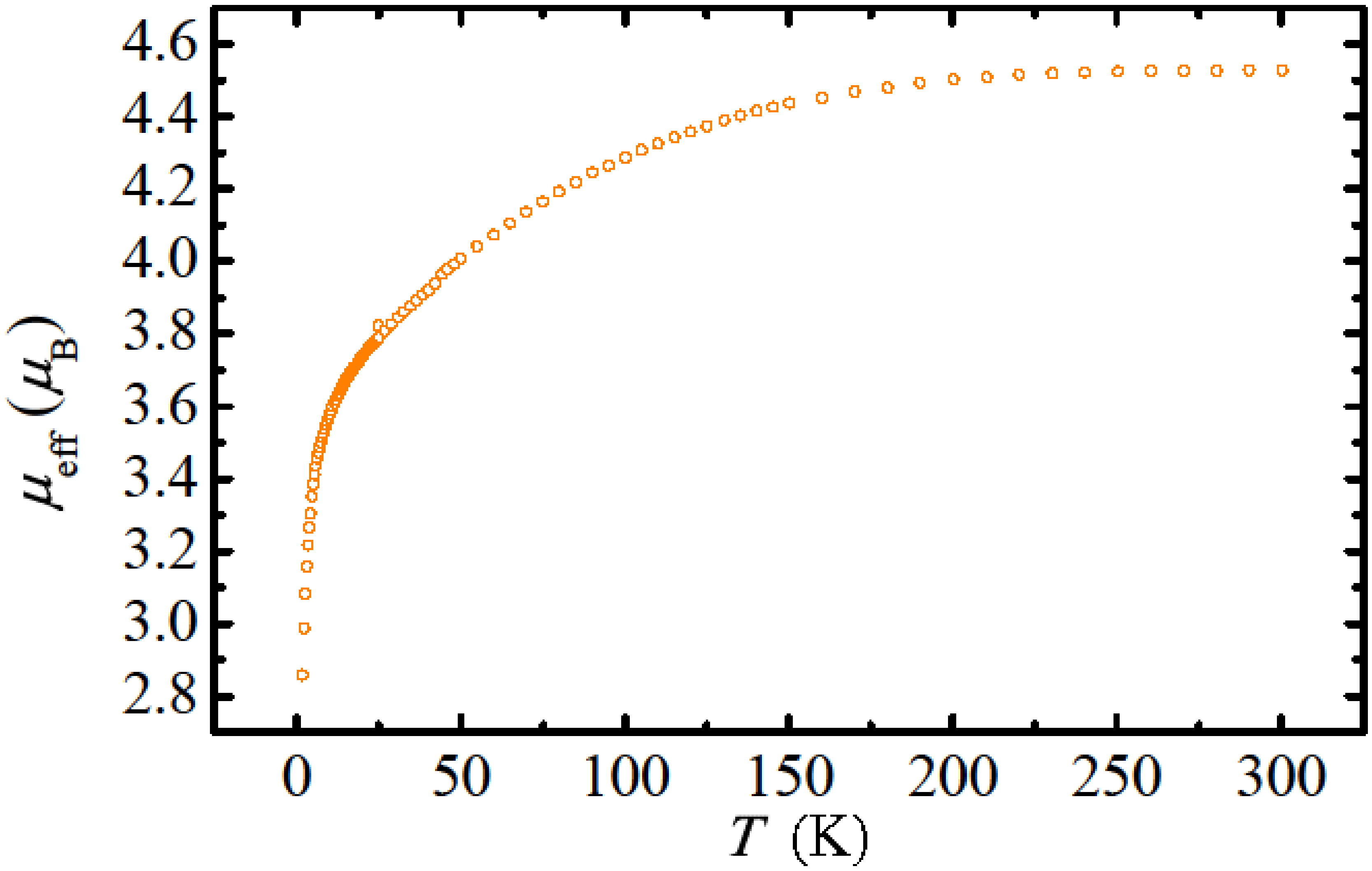

4.6
4.4
4.2
4.0
3.8
3.6
3.4
3.2
3.0
2.8
μ_{eff} (μ_B)
0
50
100
150
200
250
300
T (K)

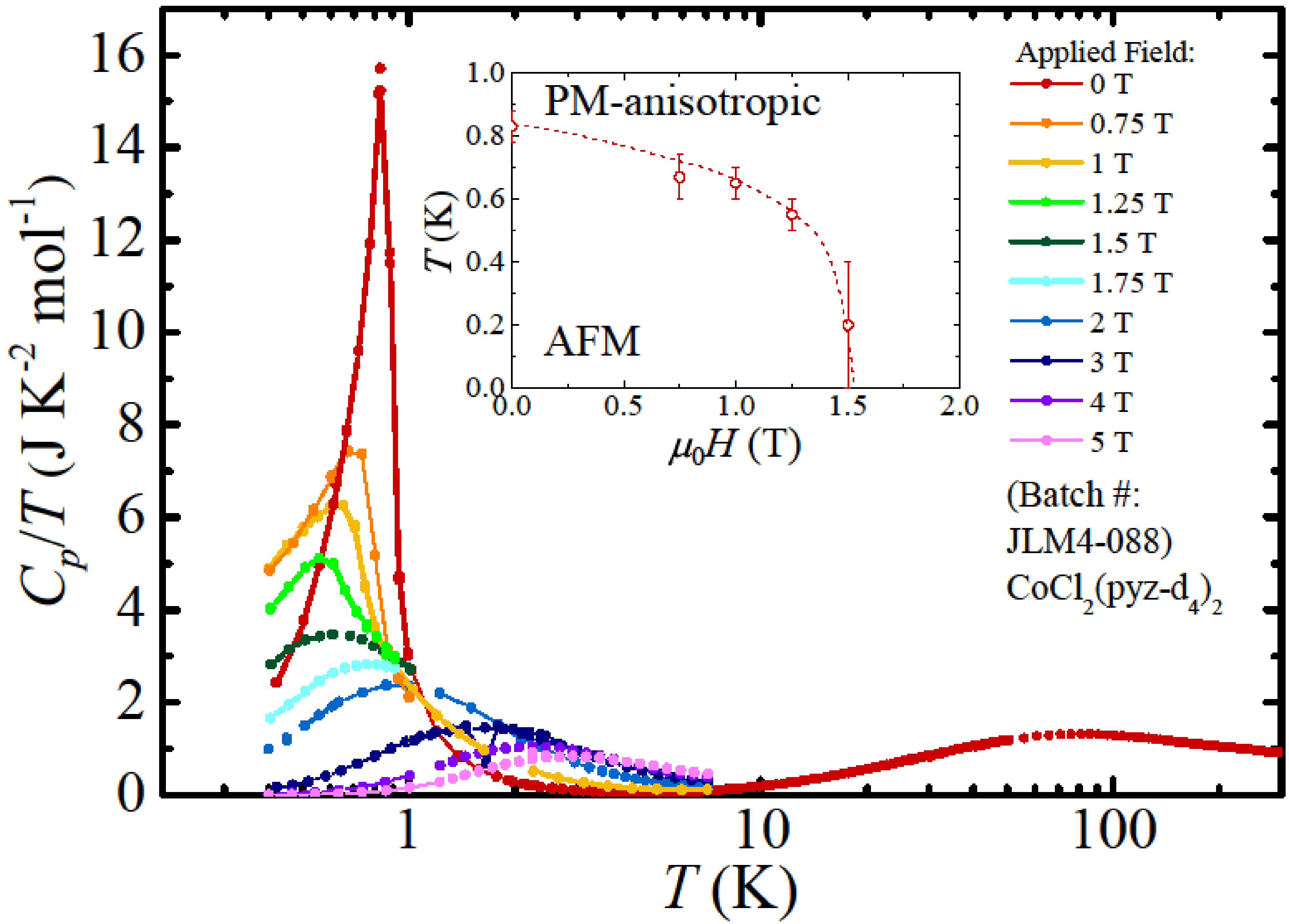

C_p/T (J K^{-2} mol^{-1})
T (K)
PM-anisotropic
AFM
T (K)
$\mu_0 H$ (T)
Applied Field:
0 T
0.75 T
1 T
1.25 T
1.5 T
1.75 T
2 T
3 T
4 T
5 T
(Batch #:
JLM4-088)
$CoCl_2(pyz\text{-}d_4)_2$

$NiBr_2pyz_2$

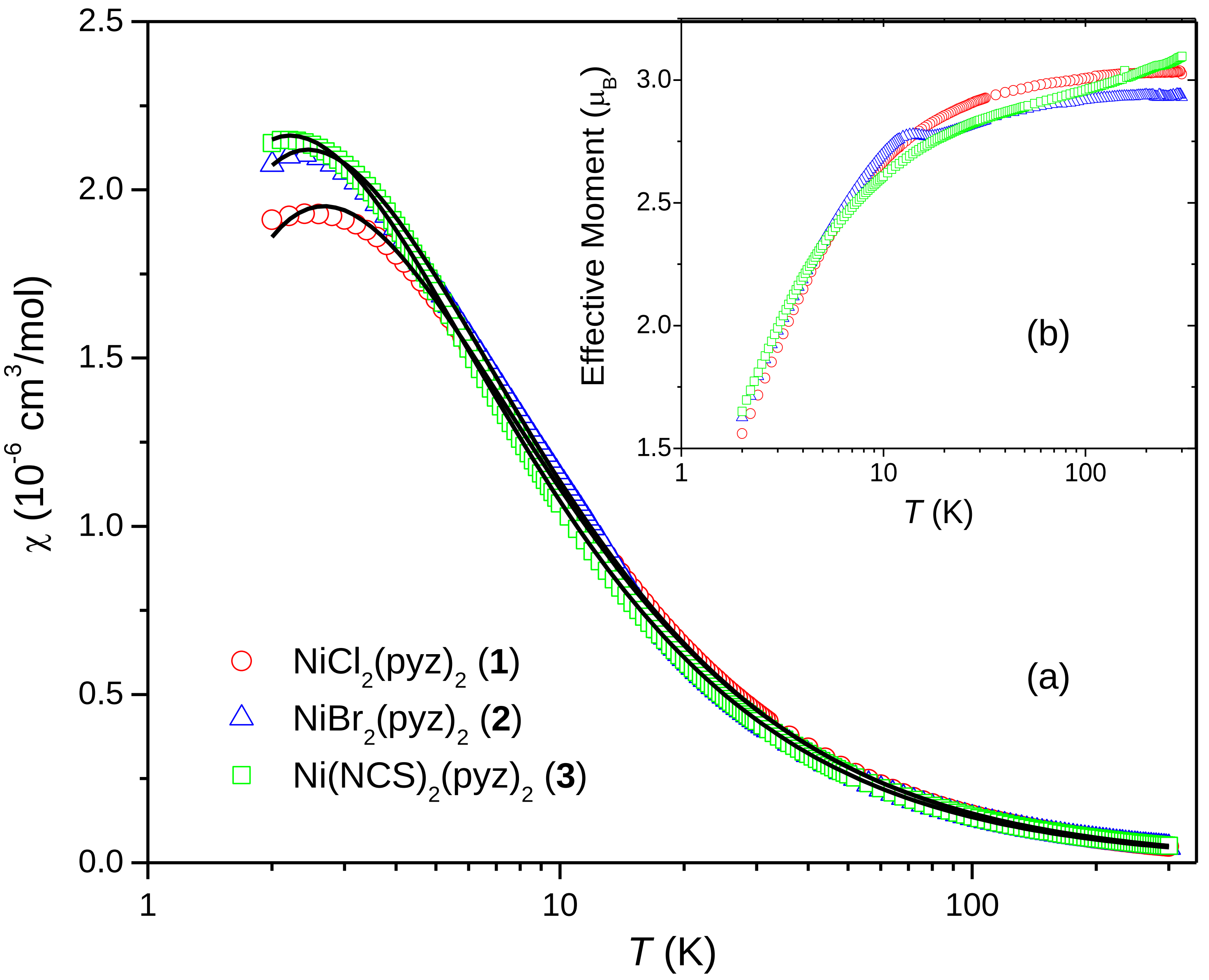

χ (10^-6 cm^3/mol)
2.5
2.0
1.5
1.0
0.5
0.0
1
10
100
T (K)
NiCl2(pyz)2 (1)
NiBr2(pyz)2 (2)
Ni(NCS)2(pyz)2 (3)
(a)
Effective Moment (μB)
3.0
2.5
2.0
1.5
1
10
100
T (K)
(b)

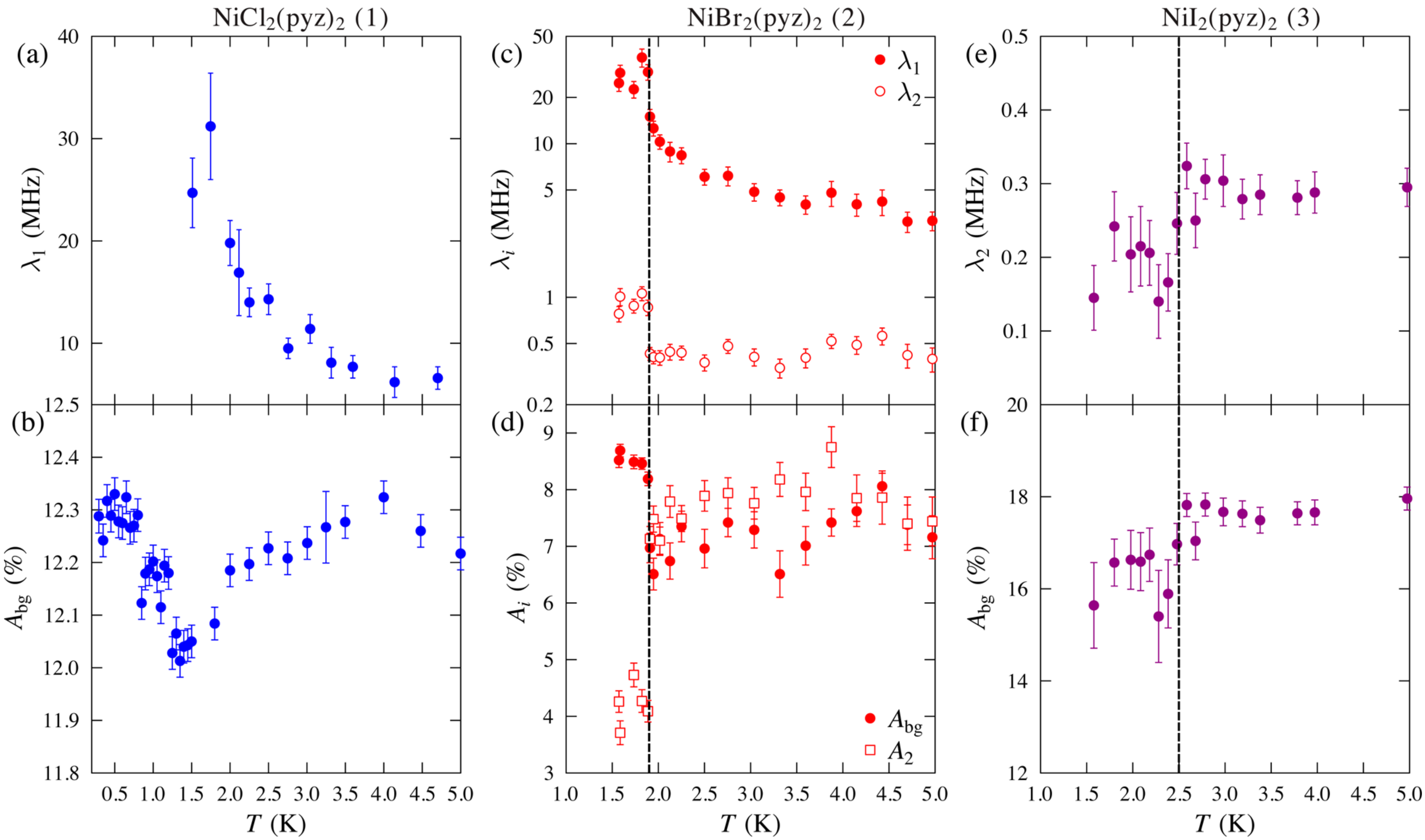

$NiCl_2(pyz)_2$ (1)
$NiBr_2(pyz)_2$ (2)
$NiI_2(pyz)_2$ (3)
(a)
(b)
(c)
(d)
(e)
(f)
λ_1 (MHz)
A_{bg} (%)
λ_i (MHz)
A_i (%)
λ_2 (MHz)
A_{bg} (%)
λ_1
λ_2
A_{bg}
A_2
T (K)
T (K)
T (K)

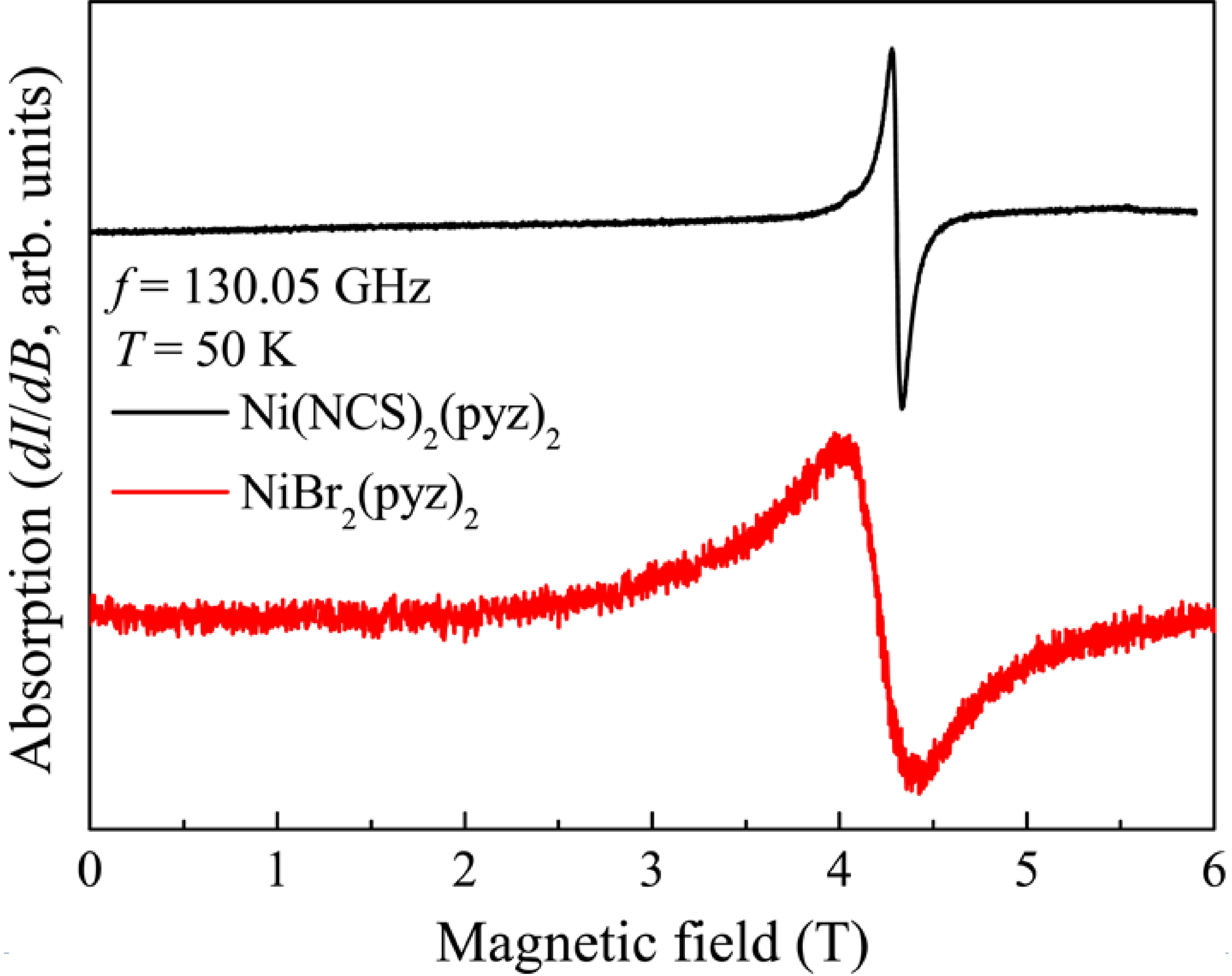

Absorption (dI/dB, arb. units)
f = 130.05 GHz
T = 50 K
$Ni(NCS)_2(pyz)_2$
$NiBr_2(pyz)_2$
0
1
2
3
4
5
6
Magnetic field (T)

Fig. 1 $NiBr_2(pyz\text{-}d_4)_2$ (Batch #: DYV01-016)

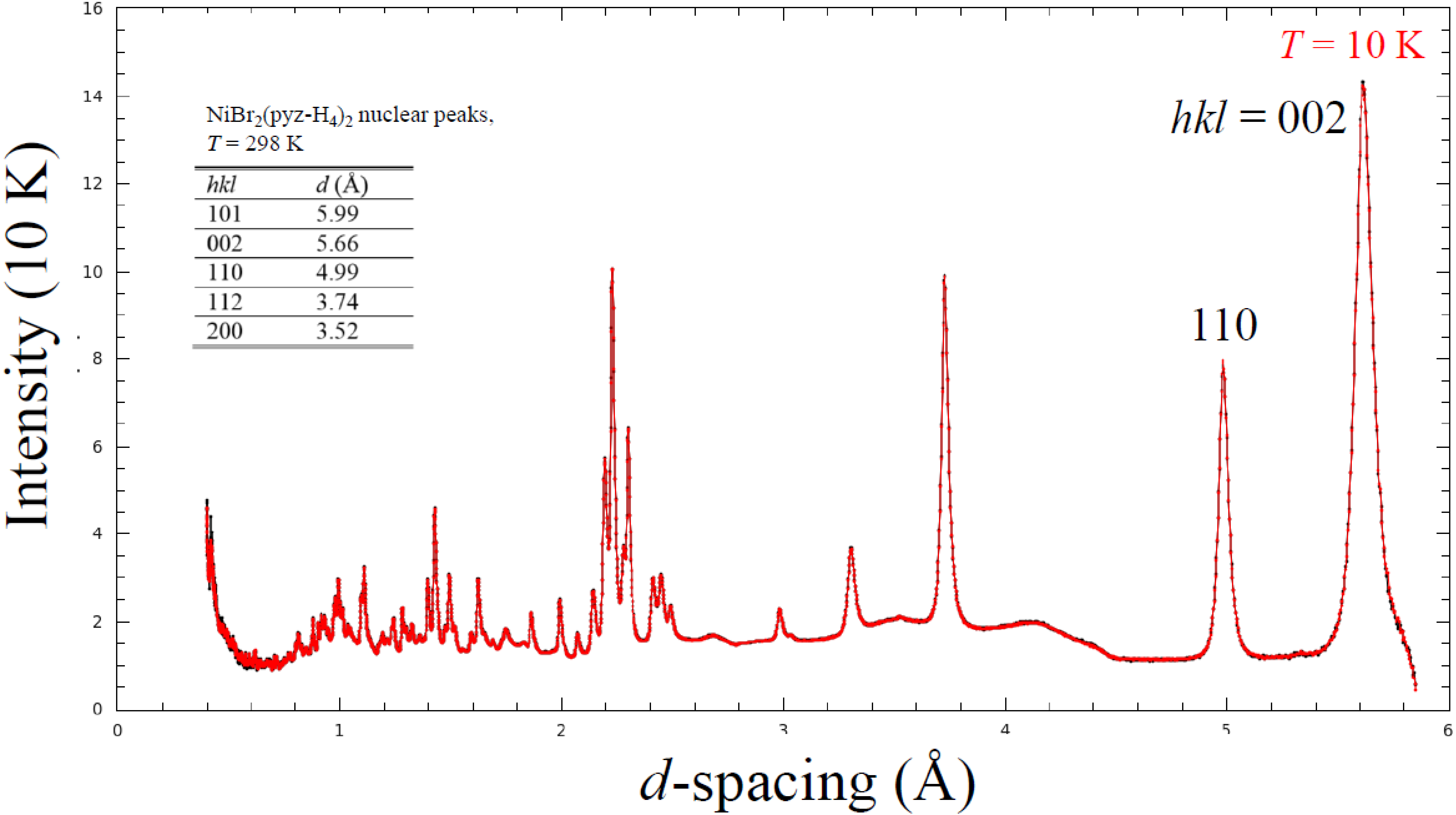

Fig. 2

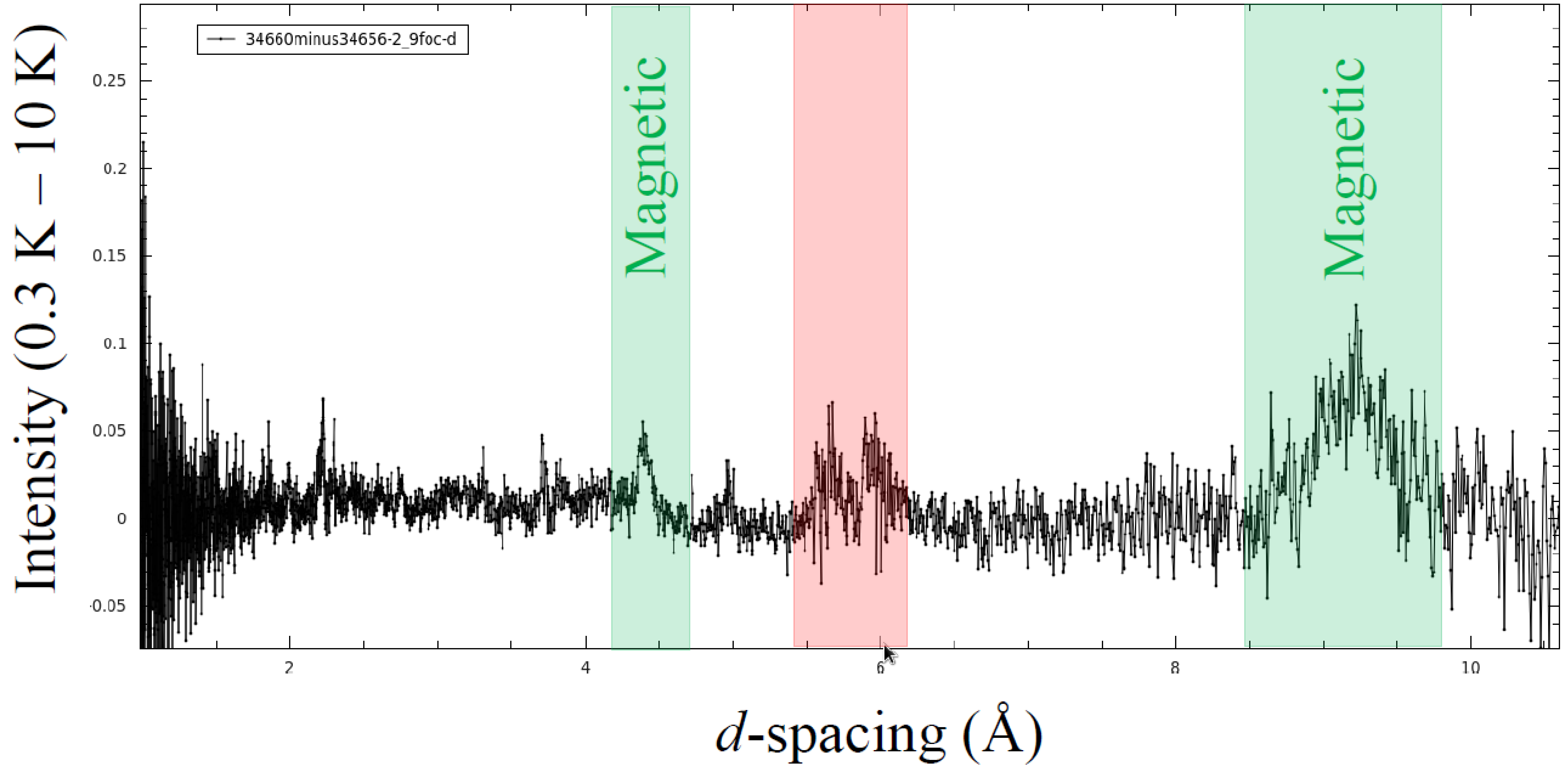

34660minus34656-2_9foc-d
Magnetic
Magnetic
Intensity (0.3 K – 10 K)
0.25
0.2
0.15
0.1
0.05
0
-0.05
2
4
6
8
10
d-spacing (Å)

Fig. 3

(a)

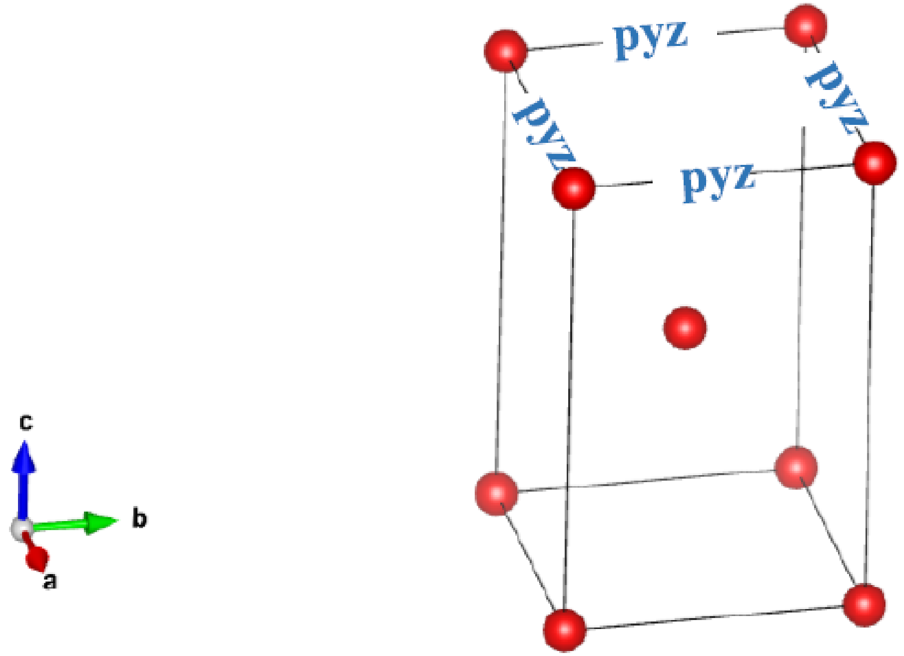

$a = b = 7.09$ Å
$c = 11.3$ Å
I4/mmm (tetragonal)
$T = 298$ K

(b)

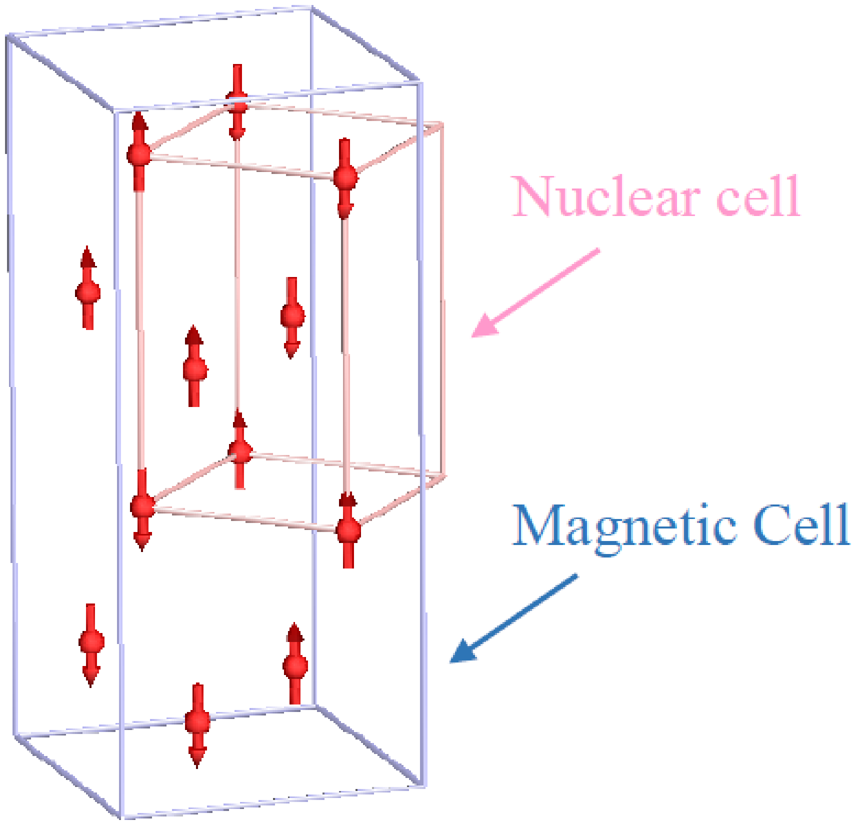

$a = b = 7.04$ Å
$c = 11.2$ Å
I4/mmm (tetragonal)
$T = 0.3$ K
$\boldsymbol{k} = [0.5\ 0.5\ 0.5]$

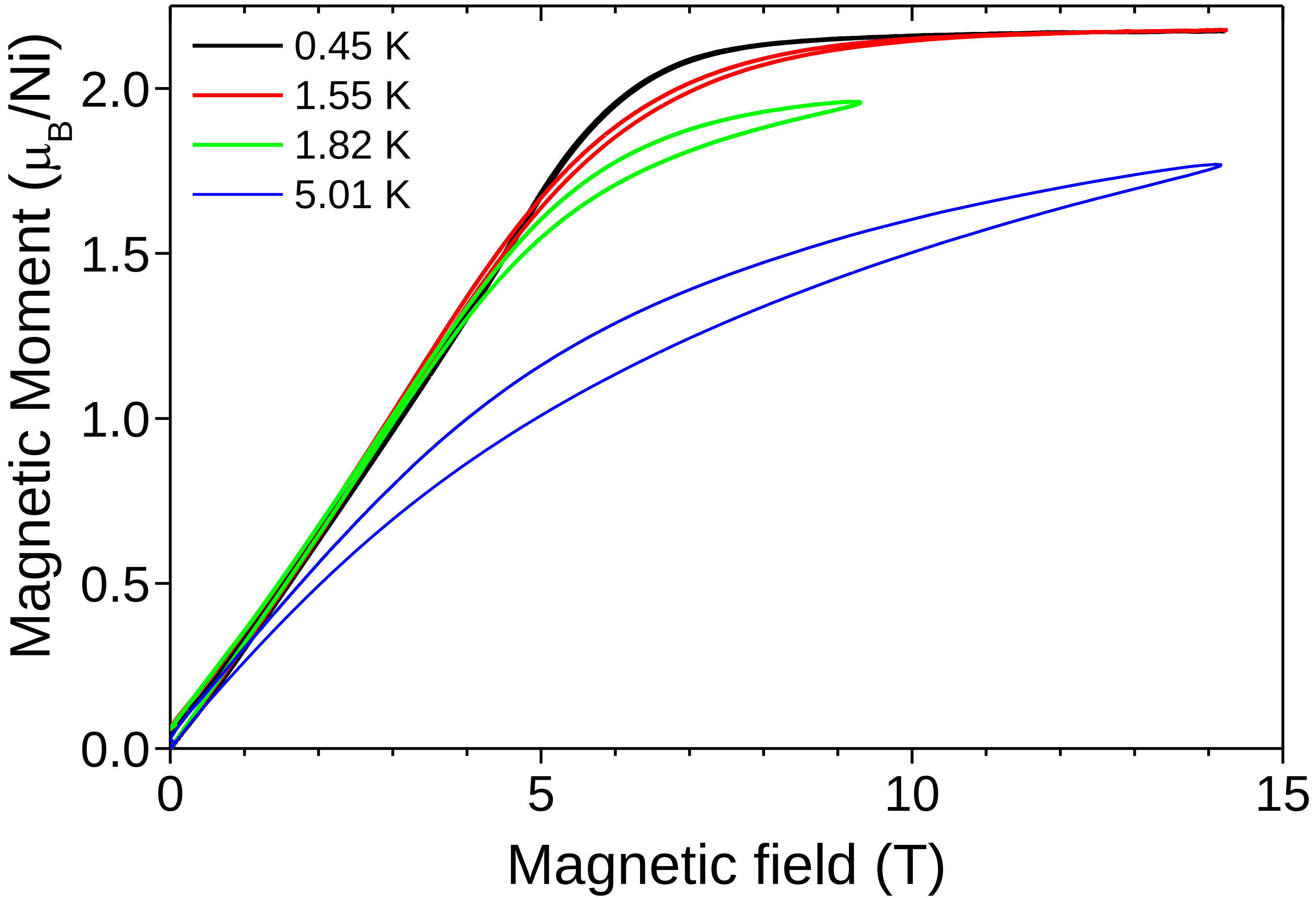

0.45 K
1.55 K
1.82 K
5.01 K
Magnetic Moment (μ_B/Ni)
0.0
0.5
1.0
1.5
2.0
0
5
10
15
Magnetic field (T)

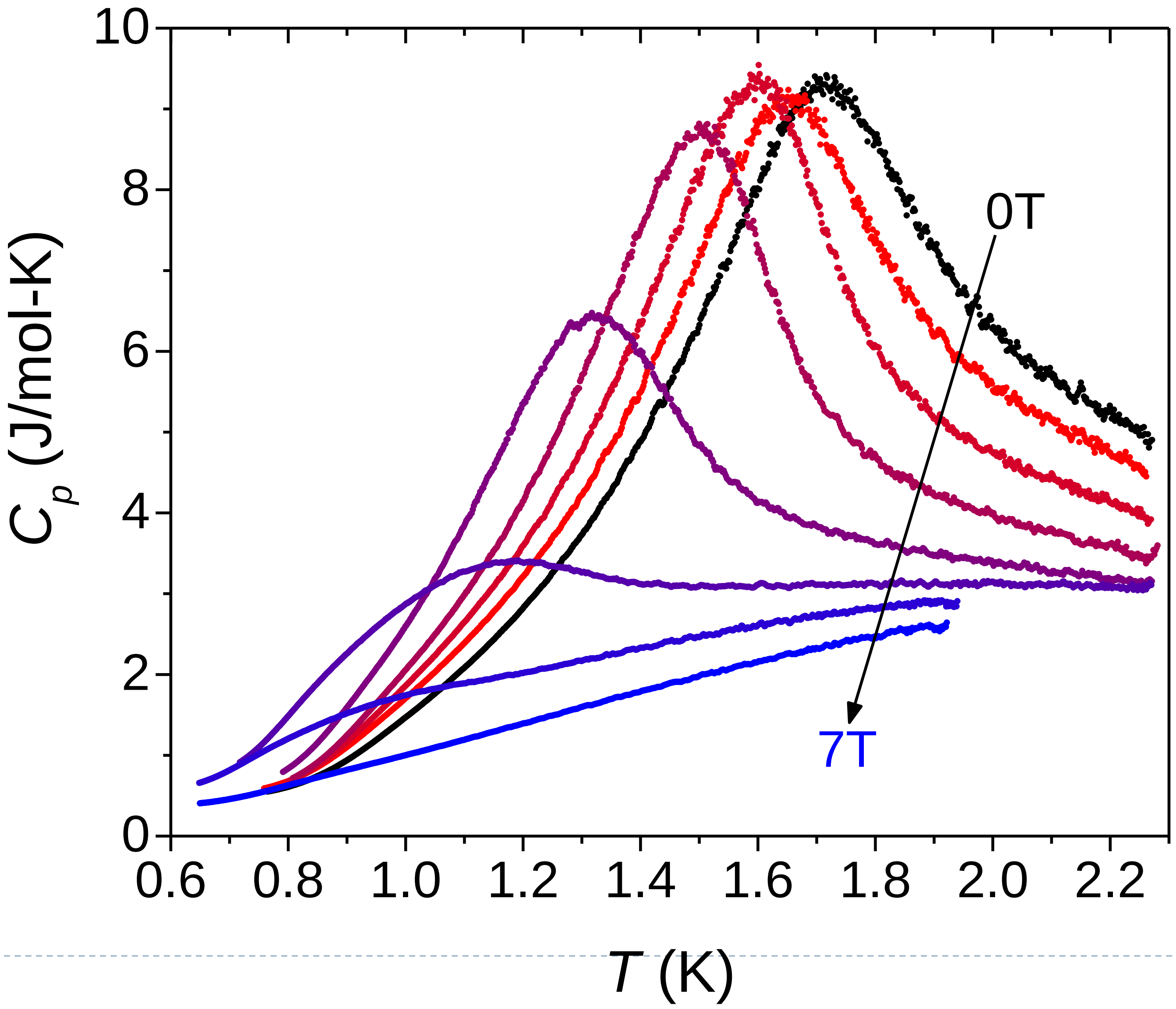

10
8
6
4
2
0
0.6
0.8
1.0
1.2
1.4
1.6
1.8
2.0
2.2
C_p (J/mol-K)
T (K)
0T
7T